University of Milan-Bicocca
School of Medicine and School of Science

PHD PROGRAM IN TRASLATIONAL
AND MOLECULAR MEDICINE
DIMET

New insights in the understanding of motor neuron disease by longitudinal brain and muscle MRI analysis and characterization of spinal cord-derived stem cells in G93A-SOD1 mouse model of amyotrophic lateral sclerosis

Dr. Stefania Marcuzzo
Matr. No.734636

Coordinator: Prof. Andrea Biondi
Tutor: Dr. Renato Mantegazza

XXV CYCLE
ACADEMIC YEAR 2011-2012

Non basta guardare,
occorre guardare con occhi
che vogliono vedere,
che credono in quello che vedono.

Galileo Galilei

TABLE OF CONTENTS

CHAPTER 3

Altered miRNA expression skews neural fate in G93A ependymal stem progenitors. Marcuzzo S, Kerlero de Rosbo N, Baggi F, Bonanno S, Barzago C, Cavalcante P, Kapetis D, Bodini M, Mantegazza R, Bernasconi P. Submitted to Stem Cells and Development.

CHAPTER 4

SUMMARY, CONCLUSIONS AND FUTURE PERSPECTIVES

References

CHAPTER 1

INTRODUCTION

1. Amyotrophic lateral sclerosis

Amyotrophic lateral sclerosis (ALS) was firstly described by Aran (Aran, 1850) and later by Charcot and Joffroy in 1869 (Charcot and Joffroy, 1869). It is a fatal progressive disorder characterized by the degeneration of upper motor neurons in the motor cortex and lower motor neurons in the brainstem and spinal cord. The name of the disease derives from Charcot's observation of a distinct myelin pallor in the lateral portions of the spinal cord, representing loss of the axon of the upper motor neurons, that descend from brain to connect directly or indirectly on the lower motor neurons in the spinal cord. The incidence of ALS in Europe is 2-3 cases per 100,000 individuals in general population (Hardiman et al., 2011). About 90% of ALS cases are sporadic (SALS) and most of them are of unknown etiology. Familial ALS (FALS) makes up the remaining cases. The SALS and FALS forms are clinically indistinguishable (Gruzman et al., 2007) and are characterized by similar pathological hallmarks, including progressive muscle weakness, atrophy, and spasticity. In FALS the time of the disease onset and duration is different. Denervation of the

respiratory muscles and diaphragm is generally the fatal event (Bourke et al., 2006). Several evidences indicate that genetic factors are involved in FALS and also in SALS (Andersen and Al-Chalabi, 2011). The 12-23% of FALS cases are caused by mutations in the superoxide dismutase 1 (SOD1) gene (Andersen and Al-Chalabi, 2011), encoding the SOD1 protein expressed in all cells and catalyzes the reduction of the superoxide anion to O^2 and H_2O_2. Since the first SOD1 missense mutations were discovered (Rosen et al., 1993), the number of know mutations has increased to more than 150 (Andersen and Al-Chalabi, 2011). Many SOD1 mutants result in the same age of onset, but in different disease progression, sites of symptom onset or disease penetrance (Andersen and Al-Chalabi, 2011). The mutations in SOD1 gene can lead to a gain of toxic function or to a loss or diminution of SOD1 detoxifying activity, causing oxidative stress through an excessive extracellular production of O^{2-} (Ilieva et al., 2009). The mutations in SOD1 gene can cause alterations in the cytoprotective machine determining the presence of cytoplasmic abnormal SOD1 protein aggregates in motor neurons and glial cells (Ilieva et al., 2009). Although ALS pathogenesis is not clearly understood, advances in genetics and molecular biology have led to the identification of a combination of several cellular mechanisms that might contribute to the selective death of motor neurons.

1.1 Pathophysiological features

1.1.1 Astrocytes and microglia damage

Astrocytes are one of the most numerous cell types in adult nervous system. Closely to motor neurons, they are responsible for supplying nutrients, buffering ions, recycling neurotransmitter precursors, and limiting motor neuron firing through rapid recovery of synaptic glutamate transport (Halassa and Haydon, 2010). Astrocytes respond to damage by activating several pathways, including a strong immunoreactivity to glial fibrillary acid protein (GFAP) and an increase in the number and size of cytoplasmatic processes (Pekny and Nilsson, 2005). Astrocyte activation was seen in the spinal cord of ALS patients and of SOD1 mutant mice (Hall et al., 1998; Levine et al., 1999; Schiffer et al., 1996; Diaz-Amarilla et al., 2011).

Astrocytes are the cell type primarily responsible for glutamate uptake. Glutamate uptake by astrocytes plays a role in regulating the activity of glutamatergic synapses. The release of glutamate from astrocytes via transporter reversal can contribute to glutamate receptor activation (Anderson and Swanson, 2000). Altered glutamate transport, that causes an excessive release of glutamate, determines the phenomenon of excitotoxicity, which is a common cellular mechanism of SALS and SOD1 mutant ALS (Haidet-Phillips et al., 2011; Fig. 1). Glutamate-mediated excitotoxicity effects have long been postulated to have an important role in motor neuron degeneration in ALS (Zeinman and Cudkowicz, 2011). The activity of excitatory amino-acid transporter 2 (EATT2), that regulates extracellular glutamate concentration, was reduced in synaptosomes derived from ALS tissue patients (Rothsen et al., 1992) and decreased in motor cortex and spinal cord of ALS patients (Fray et al., 1998; Maragaski et al., 2004; Rothstein et al., 1995; Sasaki et al., 2000) and

in spinal cord of mutant SOD1 mice (Bruijn et al., 1997). ALS mice, that expressed the human mutated SOD1 gene and are heterozygous for EATT2, developed earlier-onset disease (Pardo et al., 2006), while drugs that increase EATT2 activity extended the animal survival (Ganel et al., 2006; Rothstein et al., 2005). Another study demonstrated that by treating transgenic SOD1 mice with methionine sulfoximine, an inhibitor of glutamine synthetase, the levels of glutamine decreased by 60% and of glutamate by 30% and the lifespan of the mice was extended by 8%, with a decrease of the concentration of glutamate in the brain (Ghoddoussi et al., 2010). Recently, it was reported that the activation of Group I metabotropic glutamate receptors, implicated in the modulation of the release of glutamate, determined an abnormal glutamate release in ALS mouse model, suggesting that these receptors are implicated in the pathogenesis of ALS and that selective antagonists may be predicted for new therapeutic approaches (Giribaldi et al., 2012).

Additional, implication for a toxic astrocyte contribution in ALS has been demonstrated in cell co-culture of astrocytes from FALS and SALS patients and motor neurons (Haidet-Phillips et al., 2011). The authors revealed that the espression of inflammatory-pathway genes, investigated to identify the potential causes of the toxicity of FALS and SALS astrocytes, were similary up-regulated in both forms. Although a selective mutant SOD1 expression in astrocytes is not sufficient for disease onset (Lobsiger and Cleveland, 2007), a selective reduction of mutant SOD1 expression in astrocytes slowed disease progression.

The severity of ALS is accompanied by microglial activation, that shows a functional correlation with mutant astrocytes (Lobsiger and Cleveland, 2007; Fig. 1). Microglial cells explain functional plasticity during activation, involving changes in cell number, morphology, surface receptor expression, and production of growth factors and cytokines. These changes reflect the altered activation states of microglia induced by signals derived from motor neuron degeneration and neighboring astrocytes. Microglia exhibits an activated or deactivated M2 phenotype or a classically activated M1 phenotype (Nakamura, 2002). M1 activated phenotype is cytotoxic due to the secretion of reactive oxygen species (ROS) and proinflammatory cytockines; M2 activated or deactivated phenotype blocks proinflammatory response and produces high levels of anti-inflammatory cytokines and neurotrophic factors (Nakamura, 2002). In the ALS mouse model, microglia appears to switch from an M2 microglial phenotype observed at the beginning of the pathology, to an M1 phenotype as disease advances with increasing expression of proinflammatory cytokines, including TNF-α and IL-1β (Henkel et al., 2009). Microglia might improve motor neuron survival through the release of trophic and anti-inflammatory factors. It was reported that the treatment of microglia/motor neuron co-cultures with IL-4 suppressed M1 microglial activation promoting an M2 phenotype, reducing the release of ROS, enhancing insuline-like growth factor (IGF)-1 secretion, and improving motor neuron survival (Zhao et al., 2006). In addition, the enhanced IGF-1 secretion may ameliorate the activation state of astrocytes, promoting neuroprotection (D'Ercole and Ye, 2008). A recent study showed a crucial role of inflammatory

monocytes in the progression of ALS (Butovsky et al., 2012). Prior to disease onset, splenic Ly6Chi monocytes expressed a polarized M1 macrophage phenotype, which included increased levels of chemokine receptor CCR2. At disease onset, microglia showed an increase expression of chemokine ligand 2 (CCL2) and other chemotaxis-associated molecules, which led to the recruitment of monocytes to the central nervous system by spinal cord derived microglia. A therapy with anti-Ly6C monoclonal antibody modulated the Ly6C monocyte cytokine profile, reduced monocyte recruitment to the spinal cord, diminished neuronal death, and extended survival (Butovsky et al., 2012). The authors suggested that the recruitment of inflammatory monocytes might play an important role in ALS progression and that modulation of these cells might be a potential therapeutic approach.

1.1.2 Axonal disorganization

Alterations in axonal structure of motor neurons are well documented in SALS and FALS patients (Hirano et al., 1984; Kawamura et al., 1981) and mutant SOD1 mice (Wong et al., 1995; Fig. 1). The axons of motor neurons are characterized by accumulation of neurofilaments (Lee et al., 1994; Fig. 1), which are seen early in mutant SOD1 mice (Kong and Xu, 1998). The removal of axon neurofilaments prolonged the survival of mutant SOD1 mice (Nguyen et al., 2004). ALS motor neurons show a defect of both anterograde and retrograde axon transport (Williamson and Cleveland, 1999) before the onset of neurodegeneration. In particular, transport of vesicles was observed to

be suppressed in both anterograde and retrograde directions in ALS mice (De Vos et al., 2007); while transport of cytoskeletal elements, including neurofilaments, was reported to be slowed only in retrograde direction (Williamson and Cleveland 1999; Warita et al., 1999). Several studies suggested that mitochondrial movement could be suppressed in anterograde and retrograde directions (Magrane et al., 2009). Indeed, the expression of dynein and kinesin motor proteins, implicated in axonal transport of many organelles, including mitochondria, were altered in ALS model (Shi et al., 2009). Recently, it has been demonstrated that depletions of dynein and dynactin-1, another motor protein which regulates axonal trafficking, disrupted axonal transport, and mutations in their genes caused motor neuron degeneration in humans and rodents (Ikenaka et al., 2012). In addition, gene expression profiles indicated that dynactin-1 mRNA was down-regulated in degenerating spinal cord motor neurons of SALS patients (Ikenaka et al., 2012). Defects in kinesin-1 microtubule-binding activity and in anterograde axonal transport was correlated to activation of c-Jun *N*-terminal kinase (Ikenaka et al., 2012). This pathological mechanism caused the disruption of kinesin ability to bind microtubules, determining a failure of adequate anterograde transport (Ikenaka et al., 2012). Another recent study demonstrated that deficits in axonal transport of organelles and axon degeneration can evolve independently in the SOD1 ALS models (Marinkovic et al., 2012). In the SOD1 mouse, the axon transport deficit preceded the onset of axon degeneration; while in the SOD1 G85R ALS mouse model, motor axons degenerated, but the transport was unaffected, suggesting that axon transport deficit was not sufficient to cause

immediate motor neuron degeneration. In addition, in mice that over-expressed wild-type SOD1, axons showed chronic transport deficits, but survived (Marinkovic et al., 2012).

There is some uncertainty about the sequence of events leading to motor neuron degeneration and thus the disease. Several studies have shown dysfunction/degeneration of the neuromuscular junction in the mouse model (Frey et al., 2000; Kennel et al., 1996) when motor neuron loss is not detected yet (Chiu et al., 1995). Distal axonopathy was shown to occur early, following neuromuscular junction impairment, but before neuronal degeneration and onset of symptoms (Fischer et al., 2004). Muscle atrophy preceded this sequence of events in the mouse model (Brooks et al., 2004) and recent studies in mice expressing mutant SOD1 gene variants selectively in skeletal muscle suggested that muscle degeneration might itself lead to neurodegeneration and might cause ALS (Dupis and Echaniz-Laguna, 2010; Wong and Martin, 2010).

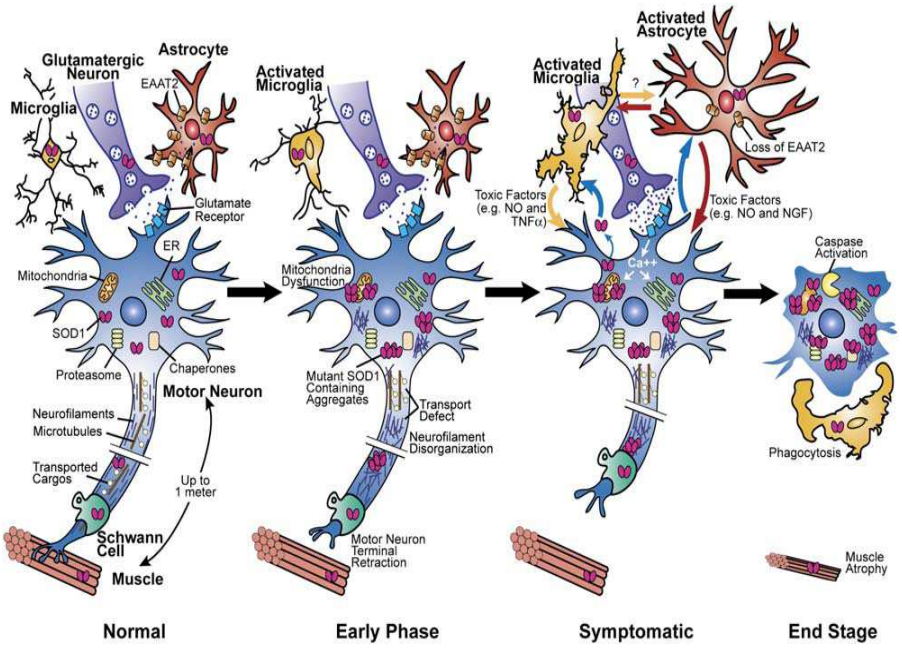

Fig.1 Evolution of motor neuron degeneration and glial activation during the course of SOD1 mutant-mediated ALS [from Neuron 2006;52:39-59].

1.1.3 Inhibition of proteasome and chaperone, endothelial stress, mitochondria damage

Pathological aggregates are characteristic of many neurodegenerative diseases, as Alzheimer, Parkinson, Huntington and ALS (Boilèe et al., 2006). To protect themselves from stress of abnormal protein aggregates all cells express a cytoprotective machinery that includes proteaosome and molecular chaperones, a family of highly conserved proteins that recognize nascent polypeptides and fold intermediates to guide proteins to their native state. Cytoplasmic abnormal SOD1 protein aggregates are observed in both SALS and FALS cases as well as in mutant SOD1 transgenic mice (Buijn et al., 1997; Gurney et al., 1994; Watanable et al., 2001). Aggregates observed in ALS patients, as well as in mouse model, contain ubiquitin (Ince et al., 1998; Watanable et al., 2001), a protein which typically targets proteins for disposal via the proteasome. It was reported that the accumulation of ubiquitinated, misfolded proteins unfavorably influenced the cytoprotective machinery causing the failure of proteasome-mediated degradation of SOD1 aggregates (Basso et al., 2006; Fig. 2).

Molecular chaperones are involved in the assembly and disassembly of multimeric complexes, traslocation of proteins across cellular membranes, and regulating vesicular transport (Bukau and Horwich 1998; Hartl and Hayer-Hartl, 2002). They have a central role in proteostasis preventing the accumulation of aggregates, as occurs in neurodegeneration such as in ALS. Hps70, a protein associated to chaperoning activity, has been observed up-regulated in chaperone in ALS models. This up-regulation influenced the failure of

cytoprotective machinery (Jain et al., 2008), suggesting that this pathogenic mechanism might be a possible therapeutic target for ALS (Jain et al., 2008; Fig. 2).

Mutant SOD1 has been observed to induce endoplasmatic reticulum (ER) stress through different pathways. Mutant aggregates were accumulated in ER membranes and in particular, in the ER-luminal polypeptide chain binding protein (BiP), a chaperone that regulate the activation of ER stress (Kikuchi et al., 2006). Another study demonstrated that mutant SOD1 inhibited ER-associated degradation and the process of eliminating proteins failed inside the ER. This phenomenon is associated with an altered retrograde transport of misfolded proteins out of the ER lumen into cytosol (Nishitoh et al., 2002).

Mitochondrial dysfunction has been reported to have an important early role in the progression of disease and has been considered a possible target for toxicity in ALS (Zeinman and Cudkowicz, 2011) (Figs. 1, 2). Mitochondria appeared vacuolated and dilated with disorganized cristae and membranes in the motor neurons and muscle in SALS and FALS patients (Zeinman and Cudkowicz, 2011). Impaired mitochondrial respiration and increased levels of misfolded proteins have been observed in spinal cord and muscle biopsies of ALS patients (Chung and Suh, 2002; Dupuis et al., 2003). The electron transport chain, which generates ATP via oxidative phosphorylation, has been demonstrated to have an accentuated or attenuated activity in mouse models (Damiano et al., 2006; Mattiazzi et al., 2002). Complex I activity has been reported elevated or reduced (Mattiazzi et al., 2002; Damiani et al., 2006). Mutant SOD1 altered

also the control of calcium homeostasis increasing the excitotoxic phenomenon that was demonstrated to be crucial for motor neuron degeneration (Damiano et al., 2006). Mitochondria are the gatekeepers of apoptosis, by opening the permeability transition pore and release of cytochrome c implicated in the cascade of caspase activation. Several studies described a relevant aspect of neuronal death associated with an activation of caspase-3 in mouse models (Li et al., 2000; Pasinelli et al., 2000) and with low levels of the antiapoptotic Bcl-2 in spinal cord tissue of ALS patients (Ekegren et al., 1999) and mutant SOD1 mice (Gonzalez de Aguilar et al., 2000). Indeed, Boston-Howes and colleagues (2006) demonstrated that in glial cells caspase-3 activation inactivated the glutamate transporter EAAT2, considered a main participant in excitotoxicity, providing an attractive mechanism which correlates mitochondrial dysfunction with excitotoxicity (Boston-Howes et al., 2006).

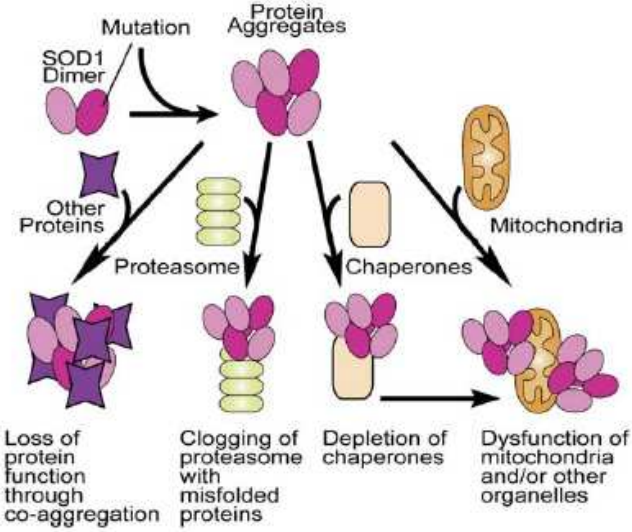

Fig. 2 Aggregate-mediated inhibition of cytoprotective machinery. [from Neuron 2006;52:39-59].

1.2 Animal model G93A-SOD1 mouse

One of the most know mutations of human SOD gene is the substitution of glycine by alanine at residue 93 (G93A) (Andersen and Al-Chalabi, 2011). Transgenic mice and rats, expressing this mutation, develop progressive motor neuron degeneration resembling human disease (Bruijn et al., 1997; Gurney et al., 1994). The G93A-SOD1 transgenic mouse has been extensively studied as an experimental model for FALS (Achilli et al., 2005). It presents clinical symptoms and neuropathological features that mimics those characteristic of FALS (Achilli et al., 2005), such as severe hind limb paralysis with atrophy of skeletal muscle. In this model, the primary symptoms are linked to the degeneration of lower motor neurons in the lumbar spinal cord and brainstem, and atrophy of the diaphragm muscles (Holzbaur et al., 2006) results in respiratory death (Tankersley et al., 2007). Mice are clinically scored for disease progression as follow: stage I (week 12-13 of age), onset of hind limb tremor and body weight; stage II, onset of hind limb paresis; stage III, severe hind limb paresis with abnormal gait; stage IV, hind limb paralysis; and stage V (week 19 of age), death for atrophy of the diaphragm muscles (Achilli et al., 2005). G93A-SOD1 mice showed numerous vacuolized motor neurons in the spinal cord in the early phase of the disease with a clear compromised blood-spinal cord barrier (Garbuzova Davis et al., 2007). Astrogliosis increased with the number of degenerating motor neurons (Levine et al., 1999). The G93A-SOD1 mouse model is excellent for many purposes. Recently, a variant of this strain expressing eight to ten mutant SOD1 genes, underwent a slower course of the disease, giving

the opportunity to study the early-stage pathological processes that characterized the disease (Acevedo-Arozena et al., 2011).

2. Spinal cord-derived stem cells

Adult neural stem cells were identified in the sub ventricular zone (SVZ) and in the subgranular zone of mammalian brain (Ming and Song, 2011). They are able to proliferate, to self renewal and to differentiate into the three different types of neural cells: neurons, astrocytes and oligodendrocytes (Ming and Song, 2011). Adult neural stem cells reside in specific cellular microenvironments or niches, which are considered as biochemical entities rather than anatomical entities because they enclosed complex signals that regulate the capacity of stem cells to proliferate, self renew and differentiate (Ming and Song, 2011).

In the 1990s, researchers identified and isolated neural stem cells from adult mammalian spinal cord (Weiss et al., 1996). Xu and colleagues (2008) demonstrated that stem cells were largely distributed in dorsal horn and central canal of rodent spinal cord and that they were more numerous in the cervical segment than in the lumbar and thoracic regions (Xu et al., 2008). These stem cells resided in a biochemical niche identified in the central ependymal zone of spinal cord (Hamilton et al; 2009). Immunohistochemical comparison of the ependymal zone of spinal cord and the SVZ niche revealed a distinct pattern of neural precursor marker expression. In particular, in the spinal cord the ependymal cells were delimited by a sub-ependymal layer, which was relatively less elaborate than that of the SVZ and

comprised of small numbers of astrocytes, oligodendrocyte progenitors and neurons. Proliferating cells surrounding, in particular, the dorsal region of the central canal, occurred in close association with PECAM-expressing blood vessels. These typically self-renewal Ki67+ proliferating cells resided within the ependymal layer and showed no evidences of a relationship to sub-ependymal cells. The dorsal region of the central canal is characterized by a sub-population of tanycyte-like cells that express markers of both ependymal cells and neural precursors, and their presence correlated with higher numbers of proliferating ependymal cells. Within the sub-ependymal region, there are GFAP expressing astrocytes, Olig2-expressing oligodendrocyte progenitors, double cortin X-expressing neuroblasts and nestin-expressing neural progenitor/stem cells. NeuN-expressing neurons are located under the sub-ependymal zone and do not proliferate. In the spinal cord, the central canal was lined with ciliated ependymal cells that expressed vimentin (Hamilton et al., 2009; Fig. 3).

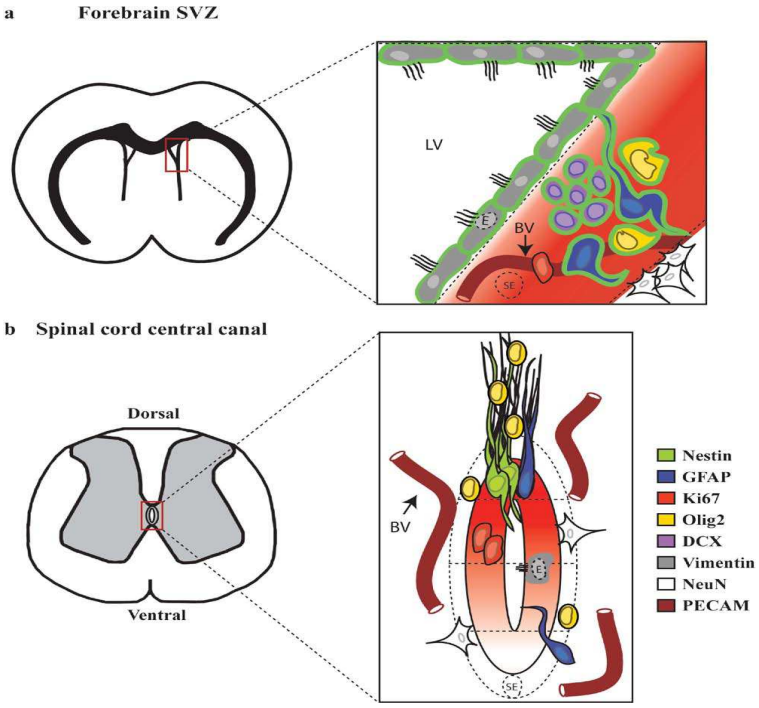

Fig. 3 Comparison of the forebrain SVZ stem cell niche and spinal cord ependymal cell niche. [from Neuroscience 2009;164:1044-1056].

Several physiological and pathological conditions, including neurodegenerative and spinal cord injury diseases, promote an extensive stem cell proliferation (Guan et al., 2007; Mothe et al., 2005). In experimental autoimmune encephalomyelitis induced in rats, stem cells not only proliferated but also migrated to the neuroinflammed area and differentiated into cells expressing neuronal markers (Danilov et al., 2006). After a trauma stem cells positive to nestin increased in the lesion site of injured rats (Foret et al., 2010). In ALS mice it was demonstrated that neurodegeneration promoted the proliferation and migration of stem cells residing (and normally quiescent) in the spinal cord (Guan et al., 2007). Stem cells migrated out the ependymal zone initially toward the dorsal horn direction and then to the ventral horn regions, where motor neurons were degenerated (Chi et al., 2005). However, as in human ALS, new mature motor neurons were not generated in G93A-SOD1 mouse spinal cord (Guan et al., 2007). The presence of stem cells in the adult spinal cord suggests that endogenous stem cell-associated mechanisms might be exploited to repair or sustain the neurodamage.

Spinal cord-derived stem cells cultured *in vitro* generate floating clonal aggregates, usually termed as neurospheres. The neurospheres are characterized by stem, progenitor and apoptotic cells and undergo a symmetric and asymmetric division (Reynolds and Rietze, 2005). The neurospheres show the capacity to proliferate and self renewal and to differentiate *in vitro* into three neural phenotypes: neurons, astrocytes and oligodendrocytes (Meletis et al., 2008). It was proposed that bone morphogenetic factors (BMPs) could regulate the proliferation and differentiation of stem cells after traumatic injury

(Xiao et al., 2010). Neurosphere cultures showed that BMP-4 promoted astrocyte differentiation from stem cells, and suppressed differentiation production of neurons and oligodendrocytes. Conversely, the inhibition of BMP-4 by Nogging decreased the ratio of astrocytes to neurons (Xiao et al., 2010). Indeed, spinal cord-derived stem cells, specifically termed as ependymal stem progenitor cells (epSPCs), isolated from injured rats, proliferated *in vitro* faster than stem cells derived from control animals. A relevant role of inflammation, on signaling pathways in stem cells after injury, has been revealed through gene expression analysis. Neurosphere cultures from spinal cord injured rats were able to differentiate into oligodendrocytes and functional motor neurons (Moreno-Manzano et al., 2010). Transplantation of undifferentiated stem cells and precursor oligodendrocytes into a spinal cord of injured rat, determined a significant recovery of motor activity. These cells were able to migrate for long distance in and around the lesion site. The endogenous modulation of these stem cells might represent a viable-cell strategy for repairing neuronal dysfunction (Moreno-Manzano et al., 2010).

Interestingly, stem cells derived from post-mortem spinal cord of SALS and FALS patients showed their multipotential capacity to differentiate *in vitro* into the three neural cell lineages (Haidet-Phillips et al., 2011). The authors (2011) demonstrated that astrocyte differentiated generated from spinal cord derived-stem cells, of both FALS and SALS patients, were similarly toxic to motor neurons obtained from mouse embryonic stem cells. The stem cells as a source of multipotent cells represent a new *in vitro* model system, to

investigate common disease mechanisms and evaluate potential therapies for SALS and FALS (Haidet-Phillips et al., 2011).

3. MicroRNAs

MicroRNAs (miRNAs) are non-coding, 18-25 nucleotide-long RNA transcripts that regulate gene expression by promoting the post-transcriptional inhibition or degradation of complementary mRNA sequences (Makeyev and Maniatis, 2008). The biogenesis of miRNAs is conserved and includes endonucleolytic cleavages by two RNase III enzymes, Drosha and Dicer (Kim, 2005; Sun et al., 2010). miRNAs are initially transcribed as a long, capped polyadenylated pri-miRNA. The Drosha complex crops the pri-miRNA into a hairpin-shaped pre-miRNA (Fig. 4). Next, exportin-5 promotes the nuclear translocation of the pre-miRNA, which is processed by the Dicer complex. The resulting miRNA:miRNA* is dissociated and the mature miRNA is incorporated into the RISC, where it functions to regulate gene silencing either by translational inhibition or by promoting the degradation of target mRNAs (Kim 2005; Sun et al., 2010; Fig. 4).

miRNAs play a crucial role in many neuronal biochemical pathways, including neuroplasticity and stress responses. Altered miRNA expression is associated with neurodegenerative disease, including ALS (De Smaele et al., 2010; Haramati et al., 2010; Satoh et al., 2010). miRNAs target and regulate the expression of particular proteins that could be crucial for disease pathogenesis. Considering that the toxic protein aggregates in neuronal populations appears to be critical to neurodegeneration, as in Alzheimer's disease, miRNA-

mediated regulation represents a new target of significant therapeutic prospects (Schonrock et al., 2010; Junn and Mouridian, 2011). Haramati and colleagues (2010) observed that miRNA activity was essential for long-term survival of postmitotic spinal motor neurons; mice that did not process miRNA in the spinal motor neuron exhibited hallmarks of spinal muscular atrophy, sclerosis of the spinal ventral horns and myofiber atrophy with signs of denervation. This study underlines the potential role of miRNA in the neurodegenerative processes (Hamarati et al., 2010). miRNAs might serve as biomarkers for neurodegenerative disease (Keller et al., 2009) including spinal cord injury; specifically, it was observed that changes in miRNA expression explained the variability in initial injury severity (Strickland et al., 2011). In multiple sclerosis, miRNA microarray analysis in blood cells from patients identified as the best biomarker of the disease miR-145, suggesting the potential role of miRNA expression profile as diagnostic biomarkers for human diseases (Keller et al., 2009). Interestingly, plasma concentrations of brain-specific miRNAs were identified as early biomarker of cerebral infarction in rats, that were generated by middle cerebral artery occlusion (Weng et al., 2011).

In ALS, disease-associated mutations in TDP-43 (Andersen and Al-Chalabi, 2011), a protein involved in the Drosha complex required for the biogenesis of miRNAs, strongly implicate miRNA dysfunction in ALS pathogenesis. It was reported that a deficiency in a skeletal muscle-specific miRNA, miR-206, accelerated disease progression in ALS mice (Williams et al., 2009). Indeed, the transcriptional repression observed in FALS and SALS motor neuron transcriptomes

(Jiang et al., 2005; Kirby et al., 2005) most likely reflected an alteration in miRNA expression. Similar transcriptional repression was observed at late-stage disease in G93A-SOD1 mice (Ferraiuolo et al., 2007).

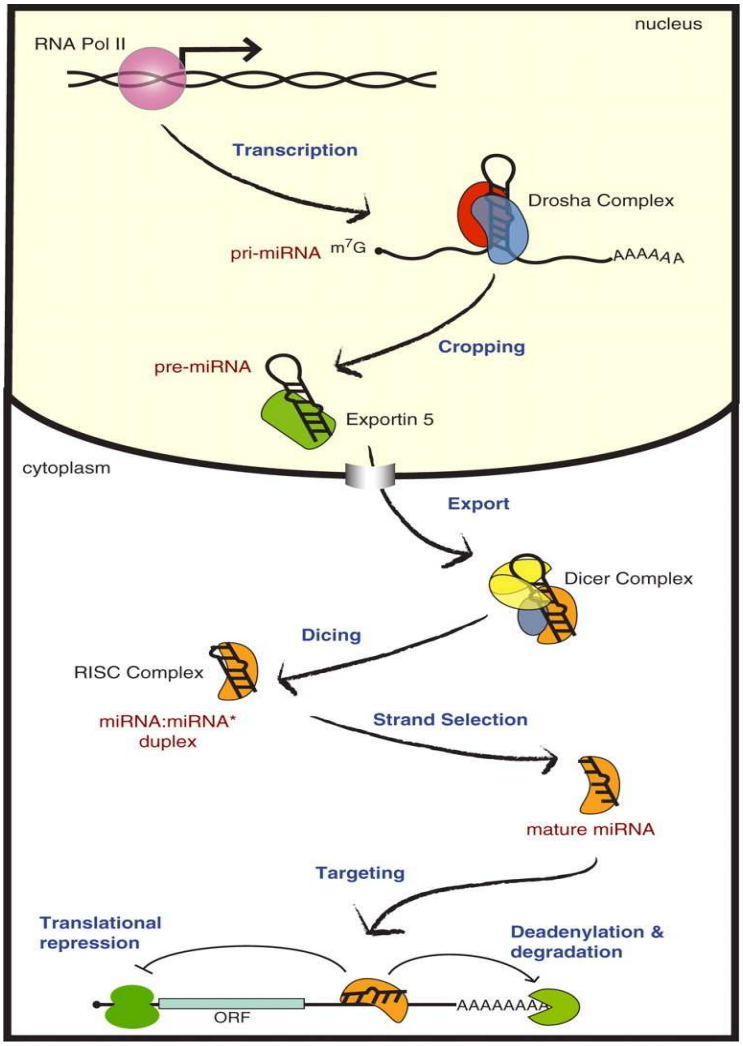

Fig. 4 miRNA biogenesis pathway. [from Journal of Biochemistry 2010;148:381-392].

3.1 microRNA-124a and-9

Several studies indicated that miRNAs play a critical role in maintenance, differentiation, and lineage commitment of stem cells (Liu and Zhao, 2009; Arnold et al., 2011). Distinct miRNAs are functionally involved in modulating neural differentiation of embryonic and adult stem cells (Krichevsky et al., 2006; Cheng et al., 2009; Shen and Temple, 2009; Zhao et al., 2009; Delaloy et al., 2010; Gao, 2010; Li and Jin, 2010; Jing et al., 2011).

miR-124a and miR-9 are highly expressed in the central nervous system. miR-124a is the most abundant miRNA in the adult brain (Lagos-Quintana et al., 2002). Cheng and colleagues (2009) demostred that miRNA-124 was up-regulated by neuroblasts in adult SVZ of mammalian brain. They found that this miRNA was an important regulator of the temporal progression of adult neurogenesis in mice. They identified the SRY-box transcription factor Sox9 as a target gene of miR-124 at the transition from the transit amplifying cell to the neuroblast stage. The over expression of Sox9 abolished neuronal differentiation, and Sox9 knockdown led to increased neuron formation (Cheng et al., 2009). miR-124a promotes neuronal differentiation and neurogenesis in vivo by down-regulating expression of Sox9 (Cheng et al., 2009; Shi et al., 2010). This miRNA was also recently shown to be expressed in microglia where it plays a role in maintaining the cells in a quiescent statein normal central nervous system (Ponomarev et al., 2012), a feature highly relevant to central nervous system diseases associated with inflammation.

miR-9 is expressed specifically in neurogenic regions of the brain during development and adulthood; it promotes neurogenesis by downregulating different suppressors of neuronal differentiation (Gao, 2010) and is upregulated during differentiation of adult stem cells in culture (Zhao et al., 2009). miR-9 promote the differentiation of mesenchymal stem cells into neurons through Notch signaling (Jing et al., 2011); it is involved in neural stem cell fate determination through a feedback regulatory loop with the nuclear receptor TLX (Zhao et al., 2009) and could coordinate proliferation and migration choices in human neural progenitor cells through targeting stathmin (Delaloy et al., 2010).

In vitro, miR-124a and miR-9 were shown to promote the neuronal phenotype during differentiation of uncommitted cells (Krichevsky et al., 2006). Brain-specific miR-124a and miR-9 were involved into neural differentiation of embryonic stem cells and their function was regulated directly or indirectly by a specific target activator of transcription (STAT) 3, a member of the STAT family cell signalling pathway responsible for cell survival and neurogenesis (Krichevsky et al., 2006). Recently, a study demonstrated that the transfection of these two neuronal miRNAs into human fibroblasts induced their conversion into neurons that exhibited functional synapses (Yoo et al., 2011).

3.2 MicroRNA-19a and -b

MiR-19a and -19b belong to the miR-19 family of the mir-17-92 cluster which has been linked to tumorigenesis (Jevnaker et al., 2011;

Olive et al., 2009). More generally, miRNAs of the mir-17-92 cluster tend to target genes involved in growth control and cell-cycle regulation (Cloonan et al., 2008). In this context, miR-19a and -19b are enriched in several stem-cell types and were shown to be part of the early commitment signature that marks a conserved stem-to-progenitor transition process (Arnold et al., 2011). Stadler and colleagues (2010) observed that these miRNAs were highly expressed in embryonic stem cells and were down regulated in all cell lines analyzed in response to early cell differentiation, suggesting that these miRNAs might be the key of differentiation processes (Stadler et al., 2010). In addition, miR-19a and 19-b were up-regulated in undifferentiated adult stem cells obtained from adipose tissue and down regulated in differentiated cells generated from the neural differentiation of the adipose derived stem cells. This study confirmed a relevant role of these miRNAs during neural differentiation processes, also in adult stem cells (Cho et al., 2011). miR-19a and -19b target cyclin D2 regulating the cellular proliferation (Lam et al., 2010), and activate the Akt–mTOR pathway, thus functionally antagonizing PTEN and promoting cell survival (Olive et al., 2009). It was also demonstrated that miR-19a and -19b down-regulated the expression of SOCS-1, a gene highly implicated in the regulation of pathways associated with modulation of the cell cycle and with cell arrest and apoptosis (Pichiorri et al., 2008).

4. Aim of the thesis

The first aim of the study was to analyze the progression of ALS, by evaluating muscle atrophy and neuronal degeneration in G93A-SOD1 mice. For this purpose, we used magnetic resonance imaging (MRI), a non-invasive neuroimaging tool that permits longitudinal examination of the same animals, to investigate changes in both brain and skeletal muscle at different phases of disease development and progression. We combined MRI investigation with muscle histological analysis and motor tests to pathological changes in the brain versus pathological changes in muscle architecture, in relation to clinical signs.

In the second part of the thesis we evaluated if the adult spinal cord of G93A-SOD1 mice was a potential source of stem cells, if the stem cells derived from G93A spinal cord had a wild-type phenotype or not and finally, if miRNA expression was altered during the neural differentiation of spinal cord-derived stem cells. For this propose, we isolated and characterized spinal cord-derived stem cells from G93A-SOD1 mice at asymptomatic and symptomatic phase of the disease and from control animals and analyzed the expression levels of four specific miRNAs, miR-124a and -9, highly expressed in the central nervous system, and miR-19a and -19b, that generally tend to target gene products involved in cell-cycle regulation, in stem cell population and in spinal cord tissue.

REFERENCES

Acevedo-Arozena A, Kalmar B, Essa S, Ricketts T, Joyce P, Kent R, Rowe C. (2011). A comprehensive assessment of the SOD1G93A low-copy transgenic mouse, which models human amyotrophic lateral sclerosis. Dis Mod Mech 4:686-70.

Achilli F, Boyle S, Kieran D, Chia R, Hafezparast M, Martin JE, Schiavo G, Greensmith L, Bickmore W, Fisher EM. (2005). The SOD1 transgene in the G93A mouse model of amyotrophic lateral sclerosis lies on distal mouse chromosome 12. Amyotroph Lateral Scler Other Motor Neuron Disord 6:111-114.

Andersen PM, A Al-Chalabi. (2011). Clinical genetics of amyotrophic lateral sclerosis: what do we really know? Nat Rev Neurol 7:603-615.

Anderson CM and Swanson RA. (2000). Astrocyte glutamate transport: Review of properties, regulation, and physiological functions. Glia 32:1-14.

Aran FA. (1850). Recherches sur une maladie non encore décrite du système musculaire (atrophie musculaire progressive) Arch Gén Méd 24:5-35. 172-214.

Arnold CP, Tan R, Zhou B, Yue SB, Schaffert S, Biggs JR, Doyonnas R, Lo MC, Perry JM, Renault VM, Sacco A, Somervaille T, Viatour P, Brunet A, Cleary ML, Li L, Sage J, Zhang DE, Blau HM, Chen C,

Chen CZ. (2011). MicroRNA programs in normal and aberrant stem and progenitor cells. Genome Res 21:798-810.

Basso M, Massignan T, Samengo G, Cheroni C, De Biasi S, Salmona M, Bendotti C, Bonetto V. (2006). Insolubile mutant SOD1 is partly oligoubiquitinated in amyotrophic lateral sclerosis mice. J Biol Chem 281:33325-35.

Boillèe S, Vande CV, Cleveland DW. (2006). ALS: A Disease of motor neurons and their nonneuronal neighbors. Neuron Review 52:39-59.

Boston-Howes W, Gibb SL, Williams EO, Pasinelli P, Brown RH, Trotti D. (2006). Caspase-3 cleaves and inactivates the glutamate transporter EAAT2. J Biol Chem 281:14076-14084.

Bourke SC, Tomlison M, Williams TL, Bullock RE, Shaw PJ, Gibson GJ. (2006). Effects of non-invasive ventilation on survival and quality of life in patients with amyotrophic lateral scelrosis: a randomized controlled trial. Lancet Neurol 5:140-147.

Brooks KJ, Hill MD, Hockings PD, Reid DG. (2004). MRI detects early hindlimb muscle atrophy in Gly93Ala superoxide dismutase-1 (G93A SOD1) transgenic mice, an animal model of familial amyotrophic lateral sclerosis. NMR Biomed 17:28-32.

Bruijn LI, Becher MW, Lee MK, Anderson KL, Jenkins NA, Copeland NG, Sisodia SS, Rothstein JD, Borchelt DR, Price DL, Cleveland DW. (1997). ALS-linked SOD1 mutant G85R mediates damage to asrocytes and promotes rapidally progressive disease with SOD1-containing inclusion. Neuron 18:327-38.

Bukau B, Horwich AL. (1998). The Hsp 70 and Hsp60 chaperone machines. Cell 92:352-366.

Butovsky O, Siddiqui S, Gabriely G, Lanser AJ, Dake B, Murugaiyan G, Doykan CE, Wu PM, Gali RR, Iyer LK, Lawson R, Berry J, Krichevsky AM, Cudkowicz ME, Weiner HL. (2012). Modulating inflammatory monocytes with a unique microRNA gene signature ameliorates murine ALS. J Clin Invest 122:3063-3087.

Charcot JM, Joffroy A. (1869). Deux cas d'atrophie musculaire progressive avec lesion de la substance grise et des faisceaux antero-lateraux de la moelle epiniere. Arch. Physiol Neurol Path 2:744-754.

Cheng LC, Pastrana E, Tavazoie M, Doetsch F. (2009). miR-124 regulates adult neurogenesis in the subventricular zone stem cell niche. Nat Neurosci 12:399-408.

Chi L, Ke Y, Luo C, Li B, Gozal D, Kalyanaraman B, Liu R. (2005). Motor Neuron Degeneration Promotes Neural Progenitor Cell Proliferation, Migration, and Neurogenesis in the Spinal Cords of Amyotrophic Lateral Sclerosis Mice. Stem Cells 24:34-43.

Chiu AY, Zhai P, Dal Canto MC, Peters TM, Kwon YW, Pratis SM, Gurney ME. (1995). Age-dependent penetrance of disease in a transgenic mouse model of familial amyotrophic lateral sclrosis. Mol Cell Neurosci 6:349-362.

Cho JAH, Park HO, Lim EH and LEE KW. (2011). MicroRNA expression profiling in neurogenesis of adipose tissue-derived stem cells. J Genet 90:81-93.

Chung MJ, Suh YL. (2002). Ultrastructural changes of mitochondrial in the skeletal muscle of patients with amytrophic lateral sclerosis. Ultrastruct Pathol 26:3-7.

Cloonan N, Brown MK, Steptoe AL, Wani S, Chan WL, Forrest AR, Kolle G, Gabrielli B, Grimmond SM. (2008). The miR-17-5p microRNA is a key regulator of the G1/S phase cell cycle transition. Genome Biol 9:127.

Damiano M, Starkov AA, Petri S, Kipiani K, Klaei M, Mattiazzi M, Flint Beal M, Manfredi G. (2006). Neural mitochondrial Ca^{2+} capacity impairment precedes the onset of motor symptoms in G93A Cu/Zn-superoxide dismutase mutant mice. L Neurochem 96:1349-1361.

Danilov AI, Covacu R, Moe MC, Langmoen IA, Johansson CB, Olsson T, Brundin L. (2006). Neurogenesis in the adult spinal cord in an experimental model of multiple sclerosis. Eur J Neurosci 23:394-400.

D'Ercole AJ, Ye P. (2008). Expanding the mind: insulin-like growth factor I and brain development. Endocrinology 149:5958-5962.

De Smaele E, Ferretti E, Gulino A. (2010). MicroRNAs as biomarkers for CNS cancer and other disorders. Brain Res 1338:100-111.

De Vos KJ, Chapman AL, Tennant ME, Manser C, Tudor EL, Lau KF, Brownlees J, Ackerley S, Shaw PJ, McLoughlin DM, Shaw CE, Leigh PN, Miller CC, Grierson AJ. (2007). Familial amyotrophic lateral sclerosis-linked SOD1 mutants perturb fast axonal transport to reduce axonal mitochondria content. Hum Mol Genet 16:2720-2728.

Delaloy C, Liu L, Lee JA, Su H, Shen F, Yang GY, Young WL, Ivey KN, Gao FB. (2010). MicroRNA-9 coordinates proliferation and migration of human embryonic stem cell-derived neural progenitors. Cell Stem Cell 6:323-335.

Diaz-Amarilla P, Olivera-Bravo S, Trias E, Cragnolini A, Martinez-Palma L, Cassina P, Beckman J, Barbeito L. (2011). Phenotypically aberrant astrocytes that promote motor neuron damage in a model of inherited amyotrophic lateral sclerosis. Proc Natl Acad Sci U S A. 108:18126-31.

Dupis L, di Scala F, Rene F, De Tapia M, Oudart H, Pradat PF, Meininger V, Loeffler JP. (2003). Up-regulation of mitochondrial

uncoupling protein 3 reveals an early muscular metabolic defect in amytrophic lateral sclerosis FASEB J 17:2091-2093.

Dupuis L, Echaniz-Laguna A.(2010). Skeletal muscle in motor neuron diseases: therapeutic target and delivery route for potential treatments. Curr Drug Targets 11:1250-1261.

Ekegren T, Grudstrom E, Lindholm D, Aquilonius SM. (1999). Upregulation of Bax protein and increased DNA degradation in ALS spinal cord motor neurons. Acta Neurol Scand 100:317-321.

Ferraiuolo L, Heath PR, Holden H, Kasher P, Kirby J, Shaw PJ. (2007). Microarray analysis of the cellular pathways involved in the adaptation to and progression of motor neuron injury in the SOD1 G93A mouse model of familial ALS. J Neurosci 27:9201-9219.

Fischer LR, Culver DG, Tennant P, Davis AA, Wang M, Castellano-Sanchez A, Khan J, Polak MA, Glass JD. (2004). Amyotrophic lateral sclerosis is a distal axonopathy: evidence in mice and man. Exp Neurol 185:232-240.

Foret A, Quertainmont R, Botman O, Bouhy D, Amabili P, Brook G, Schoenen J, Franzen R. (2010). Stem cells in adult rat spinal cord: plasticity after injury and treadmill training exercise. J Neuroch 112: 762-772.

Fray AE, Ince PG, Banner SJ, Milton ID, Usher PA, Cookson MR, Shaw PJ. (1998). The expression of the glial glutamate transport protein EAAT2 in motor neuron disease: an immunohistochemical study. Eur J Neurosci 10:2481-2489.

Frey D, Schneider C, Xu L, Borg J, Spooren W, Caroni P. (2000). Early and selective loss of neuromuscular synapse subtypes with low sprouting competence in motoneuron diseases. J Neurosci 20:2534-2542.

Ganel R, Ho T, Maragakis NJ, Jackson M, Steiner JP, Rothstein JD. (2006). Selective up-regulation of the glial Na+- dependent glutamate transport GLT1 by a neuroimmunophillin ligand results in neuroprotection. Neurobiol Dis 21:556-567.

Gao FB. (2010). Context-dependent functions of specific microRNAs in neuronal development. Neural Dev 5:25.

Garbuzova-Davis S, Saporta S, Haller E, Kolomey I, Bennet PS, Potter H, Sanberg PR. (2007). Evidences of compromised blood-spinal cord barrier in early and late symptomatic SOD1mice modelling ALS. Plos ONE 11:1-9.

Ghoddoussi F, Galloway MP, Jambekar A, Bame M , Needleman R, Brusilow WSA. (2010). Methionine sulfoximine, an inhibitor of glutamine synthetase, lowers brain glutamine and glutamate in a mouse model of ALS. J Neurol Sci 290:41-7.

Giribaldi F, Milanese M, Bonifacino T, Anna Rossi PI, Di Prisco S, Pittaluga A, Tacchetti C, Puliti A, Usai C, Bonanno G. (2012). Group I metabotropic glutamate autoreceptors induce abnormal glutamate exocytosis in a mouse model of amyotrophic lateral sclerosis. Neuropharmacology [Epub ahead of print].

Gonzalez de Aguilar JL, Gordon JW, Rene F, de Tapia M, Lutz-Bucher B, Gaiddon C, Loeffler JP. (2000). Alteration of the Bcl-x/Bax ratio in a transgenic mouse model of amyotrophic lateral sclerosis: evidence for the implication of the p53 signaling pathway. Neurobiol Dis 7:406-415.

Gruzman A, Wood WL, Alpert E, Prasad MD, Miller RG, Rothstein JD, Bowser R, Hamilton R, Wood TD, Don W Cleveland, Lingappa VR, and Liu J. (2007). Common molecular signature in SOD1 for both sporadic and familial amyotrophic lateral sclerosis. Proc Natl Acad Sci 104:12524-12529.

Guan YJ, Wang X, Wang HY, Kawagishi K, Ryu H, Huo CF, Shimony EM, Kristal BS, Kuhn HG, Friedlander RM. (2007). Increased stem cell proliferation in the spinal cord of adult amyotrophic lateral sclerosis transgenic mice. J Neurochem 102:1125-1138.

Gurney ME, Pu H, Chiu AY, Dal Canto MC, Polchow CY, Alexander DD, Caliendo J, Hentati A, Kwon YW, Deng HX. (1994). Motor

neuron degeneration in mice that express a human Cu, Zn superoxide dismutase mutation. Science 264:1772-1775.

Haidet-Phillips AM, Hester ME, Miranda CJ, Meyer K, Braun L, Frakes A, Song S, Likhite S, Murtha MJ, Foust KD, Rao M, Eagle A, Kammesheidt A, Christensen A, Mendell JR, Burghes AH, Kaspar BK. (2011). Astrocytes from familial and sporadic ALS patients are toxic to motor neurons. Nat Biotechnol 29:824-828.

Halassa MM, Haydon PG. (2010). Integrated brain circuits: astrocytic networks modulate neuronal activity and behavior. Annual Review of Physiology. 72:335-355.

Hall ED, Oostveen JA, Gurney ME. (1998). Relationship of microglia and astrocytes activation to disease onset and progression in a transgenic model of familial ALS. Glia 23:249-256.

Hamilton LK, Truong MKV, Bednarczyk MR, Aumont A, Fernandes KJL. (2009). Cellular organization of the central canal ependymal qcord Neurosci 164:1044-1056.

Haramati S, Chapnik E, Sztainberg Y, Eilam R, Zwang R, Gershoni N, McGlinn E, Heiser PW, Wills AM, Wirguin I, Rubin LL, Misawa H, Tabin CJ, Brown R, Chen A, Hornstein E. (2010). miRNA malfunction causes spinal motor neuron disease. Proc Natl Acad Sci U S A 107:13111-13116.

Haramati S, Chapnik E, Sztainberg Y, Eilam R, Zwang R, Gershoni N, McGlinn E, Heiser WP, Wills A-M, Wirguin I, Rubin LL, Misawa H, Tabin CJ, Brown R, Chen AJ, Hornstein E. (2010) miRNA malfunction causes spinal motor neuron disease. PNAS 107:1311-1316.

Hardiman O, Van den Berg LH, Kiernan MC. (2011). Clinical diagnosis and managemnt of amytrophic lateral sclerosis. Nature Rew 7:639-640.

Hartl FU, Hayer-Hartl M. (2002). Molecular chaperones in the cytosol from nascent chain to folded protein. Science 295:1852-1858.

Henkel JS, Beers DR, Zhao W, Appel SH. (2009). Microglia in ALS: The Good, The Bad, and The Resting. J Neuroimmune Pharmacol 4:389-398.

Hirano A, Donnenfeld H, Sasaki S, Nakano I. (1984). Fine structural observation of neurofilaments changes in amyotrophic lateral sclerosis. J Neuropathol Exp Neurol 43:461-470.

Holzbaur ELF, Howland DS,Weber N, Wallace K, She Y, Kwak S, Tchistiakova LA, Murphy E, Hinson J, Karim R, Tan YX, Kelley P, McGill CK,Williams G, Hobbs C, Doherty P, Zaleska MM, Pangalos MN, Walsh FS. (2006). Myostatin inhibition slows muscle atrophy in rodent models of amyotrophic lateral sclerosis. Neurobiol Dis 23:697-707.

Ikenaka K, Katsuno M, Kawai K, Ishigaki S, Tanaka F. (2012). Disruption of Axonal Transport in Motor Neuron Diseases. Int J Mol Sci 13:1225-1238.

Illieva H, Polymenidou M, Cleveland D. (2009). Non-cell autonomous toxicity in neurodegenerative disorder: ALS and beyond. J Cell Biol Review 187:761-772.

Ince PG, Tomkins J, Slade JY, Thatcher NM, Shaw PJ (1998). Amyotrophic lateral sclerosis associated with genetic abnormalities in the gene encoding Cu/Zn superoxide dismutase: molecular pathology of five new cases, and comparison with previous reports and 73 sporadic cases of ALS. J Neuropathol Exp Neurol 57:895-904.

Jain MR, Ge W, Elkabes S, Li H. (2008). Amyotrophic lateral sclerosis: protein chaperone dysfunction revealed by proteomic studies of animal models. Proteomics Clin Appl 2:670-684.

Jiang YM, Yamamoto M, Kobayashi Y, Yoshihara T, Liang Y, Terao S, Takeuchi H, Ishigaki S, Katsuno M, Adachi H, Niwa J, Tanaka F, Doyu M, Yoshida M, Hashizume Y, Sobue G. (2005). Gene expression profile of spinal motor neurons in sporadic amyotrophic lateral sclerosis. Ann Neurol 57:236-251.

Jing L, Jia Y, Lu J, Han R, Li J, Wang S, Peng T. (2011). MicroRNA-9 promotes differentiation of mouse bone mesenchymal stem cells into neurons by Notch signaling. Neuroreport 22:206-211.

Junn Mouridian. (2011). MicroRNAs in neurodegenerative disease and the therapeutic potential. Pharm and Ther 133:142-150.

Kawamura Y, Dyck PJ, Shimono M, Okazaki H, Tateishi J, Doi H. (1981). Morphometric comparison of the vulnerability of peripheral motor and sensory neurons in amyotrophic lateral sclerosis. J Neuropathol Exp Neurol 40:667-675.

Keller A, Leidinger P, Lange J, Borries A, Schroes H, Scheffler M, Lenhof HP, Ruprecht K, Meese E. (2009). Multiple sclerosis: microRNA expression profiles accurately differentiate patients with relapsing-remitting disease from healthy controls. PLOSone 4:1-6.

Kennel PF, Finiels F, Revah F, Mallet J. (1996). Neuromuscular function impairment is not caused by motor neurone loss in FALS mice: an electromyographic study. Neuroreport 7:1427-1431.

Kikuchi H, Almer G, Yamashita S, Guegan C, Nagai M, Xu Z, Sosunov AA, McKhann GMI, Przedborski S. (2006). Spinal cord endoplasmic reticulum stress associated with a microsomal accumulation of mutant superoxide dismutase-1 in an ALS model. Proc Natl Acad Sci 103:6025-6030.

Kim VN. (2005). MicroRNA biogenesis: coordinated cropping and dicing. Nat rev Mol Cell Biol 6:376-385.

Kirby J, Halligan E, Baptista MJ, Allen S, Heath PR, Holden H, Barber SC, Loynes CA, Wood-Allum CA, Lunec J, Shaw PJ. (2005). Mutant SOD1 alters the motor neuronal transcriptome: implications for familial ALS. Brain 128:1686-1706.

Kong J, Xu Z. (1998). Massive mitochondrial degeneration in motor neurons triggers the onset of amyotrophic lateral sclerosis in mice expressing a mutant SOD1. J Neurosci 18:3241-3250.

Krichevsky AM, Sonntag KC, Isacson O, Kosik KS. (2006). Specific microRNAs modulate embryonic stem cell-derived neurogenesis. Stem Cells 24:857-864.

Lagos-Quintana M, Rauhut R, Yalcin A, Meyer J, Lendeckel W, Tuschl T. (2002). Identification of tissue-specific microRNAs from mouse. Curr Biol 12:735-739.

Lam QL, Wang S, Ko OK, Kincade PW, Lu L. (2010). Leptin signaling maintains B-cell homeostasis via induction of Bcl-2 and Cyclin D1. Proc Natl Acad Sci U S A 107:13812-13817.

Lee MK, Marszalek JR, Cleveland DW. (1994). A mutant neurofilament subunit causes massive, selective motor neuron death: Implications for the pathogenesis of human motor neuron disease. Neuron 13:975-988.

Levine JB, Kong J, Nadler M and Xu Z. (1999). Astrocytes interact intimately with degenerating motor neurons in mouse amytrophic lateral sclerosis (ALS). Glia 28:215-224.

Li M, Ona VO, Guegan C, Chen M, Jackson-Lewis V, Andrews LJ, Oiszewski AJ, Stieg PE, Lee JP, Przedborski S, Friedlander RM (2000). Functional role of caspase-1 and caspase-3 in an ALS transgenic mouse model. Science 288:335-339.

Li X, Jin P. (2010) Roles of small regulatory RNAs in determining neuronal identity. Nat Rev Neurosci 11:329-338.

Liu C, Zhao X. (2009). MicroRNAs in adult and embryonic neurogenesis. Neuromolecular Med 11:141-152.

Lobsiger CS and Cleveland DW. (2007). Glial cells as intrinsic components of non-cell-autonomous neurodegenerative disease. Nat Neurosci Review 10:1355-60.

Magrane J, Manfredi G. (2009). Mitochondrial function, morphology, and axonal transport in amyotrophic lateral sclerosis. Antioxid Redox Signal 11:1615-1626.

Makeyev EV, Maniatis T. (2008). Multilevel regulation of gene expression by microRNAs. Science 319: 1789-1790.

Maragakis NJ, Dykes-Hoberg M, Rothstein JD. (2004). Altered expression of the glutamate transport EAAT2b in neurological disease. Ann Neurol 55:469-477.

Marinkovic P, Reutera MS, Brilla MS, Godinhoa L, Kerschensteinerb M, Misgelda T. (2012). Axonal transport deficits and degeneration can evolve independently in mouse models of amyotrophic lateral sclerosis. PNAS 109:4296-4301.

Mattiazzi M, D'Aurello M, Gajewski CD, Martushova K, Kiaei M, Beal MF, Manfredi G. (2002). Mutated human SOD1 causes dysfunction of oxidative phosphorylation in mitochondria of transgenic mice. J Biol Chem 277:29626-29633.

Meletis K, Barnabè-Heider F, Carlèn M, Evergen E, Tomilin N, Shupliakov O, Frisèn J. (2008). Spinal cord injury reveals multineage differentiation of ependymal cells. PLOSbiology 6:e182.

Ming Guo-li, Song H. (2011). Adult neurogenesis in the mammalian brain: significant answers and significant questions. Neuron Review 70:687-702.

Mothe AJ, Tator CH. (2005). Proliferation, migration, and differentiation of endogenous ependymal region stem/progenitor cells following minimal spinal cord injury in the adult rat. Neurosci. 131:177-87.

Moreno-Manzano V, Rodríguez-Jiménez FJ, García-Roselló M, Laínez S, Erceg S, Calvo MT, Ronaghi M, Lloret M, Planells-Cases R, Sánchez-Puelles JM and Stojkovic M. (2009). Activated spinal cord ependymal stem cells rescue neurological function. Stem Cells 27:733-743.

Nakamura Y. (2002). Regulating factors for microglial activation. Biol. Pharm Bull 25:945-953.

Nguyen MD, D'Aigle T, Gowing G, Julien JP, Rivest S. (2004). Exacerbation of motor neuron disease by chronic stimulation of innate immunity in a mouse model of amyotrophic lateral sclerosis. J Neurosci 24:1340-1349.

Nishitoh H, Matsuzawa A, Tobiume K, Saegusa K, Takeda K, Inoue K, Hori S, Kakizuka A, Ichijo H. (2002). ASK1 is essential for endoplasmic reticulum stress-induced neuronal cell death triggered by expanded polyglutamine repeats. Genes & Dev 16:1345-1355.

Olive V, Bennett MJ, Walker JC, Ma C, Jiang I, Cordon-Cardo C, Li QJ, Lowe SW, Hannon GJ, He L. (2009). miR-19 is a key oncogenic component of mir-17-92. Genes Dev 23:2839-2849.

Pardo AC, Wong V, Benson LM, Dykes M, Tanaka K, Rothstein JD, Maragakis NJ. (2006). Loss of the astrocytes glutamate transport GLT1 modifies disease in SOD1(G93A) mice. Exp Neurol 201:120-130.

Pasinelli P, Houseweart MK, Brown RH, Cleveland DW. (2000). Caspase-1 and -3 are sequentially activated in motor neuron death in Cu/Zn superoxide dismutase-mediated familial amyotrophic lateral sclerosis. Proc Natl Acad Sci USA 97:13901-13906.

Penky M, Nilsson M. (2005). Astrocyte activation and reactive gliosis. Glia 50:427-434.

Pichiorri F, Suh SS, Ladetto M, Kuehl M, Palumbo T, Drandi D, Taccioli C, Zanesi N, Alder H, Hagan JP, Munker R, Volinia S, Boccadoro M, Garzon R, Palumbo A, Aqeilan RI, Croce CM. (2008). MicroRNAs regulate critical genes associated with multiple myeloma pathogenesis. Proc Natl Acad Sci U S A 105:12885-12890.

Ponomarev ED, Veremeyko T, Weiner HL. (2012). MicroRNAs are universal regulators of differentiation, activation, and polarization of microglia and macrophages in normal and diseased CNS. Glia doi:10.1002/glia.22363.

Reynolds BA, RL Rietze. (2005). Neural stem cells and neurospheres-re-evaluating the relationship. Nat Methods 2:333-336.

Rosen DR, Siddique T, Patterson D, Figlewicz DA, Sapp P, Hentati A, Donaldson D, Goto J, O'Regan JP, Deng HX. (1993). Mutations in Cu/Zn superoxide dismutase gene are associated with familial amyotrophic lateral sclerosis. Nature 362:59-62.

Rothstein JD, Martin LJ, Kuncl RW. (1992). Decreased glutamate transport by the brain and spinal cord in amytrophic lateral sclerosis. N Engl J Med 326:1464-1468.

Rothstein JD, Van Kammen M, Levely AI, Martin LJ, Kuncl RW. (1995). Selective loss of glial glutamate transport GLT-1 in amytrophic lateral sclerosis. Ann Neurol 38:73-84.

Rothstein JD, Patel S, Regan MR, Haenggel C, Huang YH, Bergles DE, Jin L, Dykes Hoberg M, Vidensky S, Chung DS. (2005). Beta-lactam antibiotics after neuroprotection by increasing glutamate transport expression. Nature 433:73-77.

Sasaki S, Komori T, Iwata M. (2000). Excitatory amino acid transport 1 and 2 immunoreactivity in the spinal cord in amyotrophic lateral sclerosis. Acta Neuropahol 100:138-144.

Satoh J. (2010). MicroRNAs and their therapeutic potential for human diseases: aberrant microRNA expression in Alzheimer's disease brains. J Pharmacol Sci 114:269-275.

Schonrock N, Ke DY, Humphreys D, Staufenbiel M, Ittner LM, Preiss T, Gotz J. (2010). NeuronalmicroRNA deregulation in response to Alzheimer’s disease amyloid-β. PLOS 5:e11070.

Shen Q, Temple S. (2009). Fine control: microRNA regulation of adult neurogenesis. Nat Neurosci 12:369-370.

Shi P, Gal J, Kwinter DM, Liu X, Zhu H. (2009). Mitochondrial dysfunction in amyotrophic lateral sclerosis. Biochim Biophys Acta 1802:45-51.

Shi Y, Zhao X, Hsieh J, Wichterle H, Impey S, Banerjee S, Neveu P, Kosik KS. (2010). MicroRNA regulation of neural stem cells and neurogenesis. J Neurosci 30:14931-14936.

Shiffer D, Cordera S, Cavalla P, Migheli A. (1996). Reactive astrogliosis of the spinal cord in amytrophic lateral sclerosis. J Neurol sci 139:27-33.

Stadler B, Ivanovska I, Mehta K, Song S, Nelson A, Tan Y, Mathieu J, Darby C, Blau CA, Ware C, Peters G, Miller DG, Shen L, Cleary MA, Ruohola-Baker H. (2010). Characterization of microRNAs involved in embryonic stem cell states. Stem Cells Dev 19:935-950.

Strickland RE, Hook MA, Balaramn S, Huie JR, Garu JW, Miranda RC. (2011). microRNA dysregulation following spinal cord contusion: implication forneural plasticity and repair. Neurosci 186:146-160.

Sun W, Li JY-S, Huang H-D, Shyy JY-J, Chien S. (2010). microRNA: a master regulator of cellular processes for bioengineering system. Annu Rev Biomed Eng 12:1-27.

Tankersley CG, Haenggeli C, Rothstein JD. (2007). Respiratory impairment in a mouse model of amyotrophic lateral sclerosis. J Appl Physiol 102:926-932.

Xiao Q, Du Y, Wu W, Yip HK. (2010). Bone morphogenetic proteins mediate cellular response and, together with Noggin regulate astrocytes differentiation after spinal cord injury. Exp Neurol 221:353-366.

Xu R, Wu C, Tao Y, Yi J, Yang Y, Zhang X, Liu R. (2008). Nestin-positive cells in the spinal cord: a potential source of neural stem cells. J Internal J Devel Neurosci 26:813-820.

Yoo AS, Sun AX, Li L, Shcheglovitov A, Portmann T, LiY, Lee-Messer C, Dolmetsch RE, Tsien RW, Crabtree GR. (2011). MicroRNA-mediated conversion of human fibroblasts to neurons, Nature 476:228-231.

Warita H, Itoyama Y, Abe K. (1999). Selective impairment of fast anterograde axonal transport in the peripheral nerves of asymptomatic transgenic mice with a G93A mutant SOD1 gene. Brain Research 819:120-131.

Watanable M, Dykes-Hoberg M, Culotta VC, Price DL, Wong PC, Rothstein JD. (2001). Histological evidence of protein aggregation in mutant SOD1 transgenic mice and in amyotrophic lateral sclerosis neural tissues. Neurobiol Dis 8:933-941.

Weiss S, Christine D, Jennifer H, Wohl C, Wheatley M, Peterson AC, Reynolds B. (1996). Multipotent CNS stem cells are present in the adult mammalian spinal cord and ventricular neuroaxis. J Neurosci 16:7599-7609.

Weng H, Shen C, Hirokawa G, Ji X, Takahashi R, Shimada K, Kishimoto C, Iwai N. (2011). Plasma miR-124 as a biomarker for cerebral infarction. Biom Res 32:135-141.

Williams AH, Valdez G, Moresi V, Qi X, McAnally J, Elliott JL, Bassel-Duby R, Sanes JR, Olson EN. (2009). MicroRNA-206 delays ALS progression and promotes regeneration of neuromuscular synapses in mice. Science 326:1549-1554.

Williamson TL, Cleveland DW. (1999). Slowing of axonal transport is a very early event in the toxicity of ALS-linked SOD1 mutants to motor neurons. Nat neurosci 2:50-56.

Wong M, Martin LJ (2010). Skeletal muscle-restricted expression of human SOD1 causes motor neuron degeneration in transgenic mice. Hum Mol Genet 19:2284-2302.

Wong PC, Pardo CA, Borchelt DR, Lee MK, Copeland NG, Jenkins NA, Sisodia SS, Cleveland DW, Price DL. (1995). An adverse property of familial ALS-linked SOD1 mutation causes motor neuron disease characterized by vacuolar degeneration of mitichondria. Neuron 14:1105-1116.

Zeinman L, Cudkowicz M. (2011). Emerging targets and treatments in amytrophic lateral sclerosis. Lancet Review 10:481-490.

Zhao W, Xie W, Xiao Q, Beers DR, Appel SH. (2006). Protective effects of an anti-inflammatory cytokine, interleukin-4, on motoneuron toxicity induced by activated microglia. J Neurochem 99:1176-1187.

Zhao C, Sun G, Li S, Shi Y. (2009). A feedback regulatory loop involving microRNA-9 and nuclear receptor TLX in neural stem cell fate determination. Nat Struct Mol Biol 16:365-371.

.

CHAPTER 2

Hind limb muscle atrophy precedes cerebral neuronal degeneration in G93A-SOD1 mouse model of amyotrophic lateral sclerosis: A longitudinal MRI study.

Stefania Marcuzzo, Ileana Zucca, Alfonso Mastropietro, Nicole Kerlero de Rosbo, Paola Cavalcante, Silvia Tartari, Silvia Bonanno, Lorenzo Preite, Renato Mantegazza, Pia Bernasconi.

Published: Experimental Neurology 2011;231:30-7.

Abstract

Amyotrophic lateral sclerosis (ALS) is a progressive, fatal, neurodegenerative disorder caused by the degeneration of motor neurons in the CNS, which results in complete paralysis of skeletal muscles. Recent experimental studies have suggested that the disease could initiate in skeletal muscle, rather than in the motor neurons. To establish the timeframe of motor neuron degeneration in relation to muscle atrophy in motor neuron disease, we have used MRI to monitor changes throughout disease in brain and skeletal muscle of G93A-SOD1 mice, a purported model of ALS. Longitudinal MRI examination of the same animals indicated that muscle volume in the G93A-SOD1 mice was significantly reduced from as early as week 8 of life, 4 weeks prior to clinical onset. Progressive muscle atrophy from week 8 onwards was confirmed by histological analysis. In contrast, brain MRI indicated that neurodegeneration occurs later in G93A-SOD1 mice, with hyperintensity MRI signals detected only at weeks 10–18. Neurodegenerative changes were observed only in the

motor nuclei areas of the brainstem; MRI changes indicative of neurodegeneration were not detected in the motor cortex where first motor neurons originate, even at the late disease stage. This longitudinal MRI study establishes unequivocally that, in the experimental murine model of ALS, muscle degeneration occurs before any evidence of neurodegeneration and clinical signs, supporting the postulate that motor neuron disease can initiate from muscle damage and result from retrograde dying-back of the motor neurons.

Introduction

Amyotrophic lateral sclerosis (ALS) is the most common form of motor neuron disease. ALS is a progressive, fatal, neurodegenerative disorder caused by the degeneration of motor neurons in the spinal cord, the brainstem, and the motor cortex. It leads to complete paralysis of skeletal muscles and premature death, usually from respiratory failure. ALS can occur in two different forms: sporadic ALS in about 90% of cases, mostly of unknown etiology, and familial ALS (FALS) in the remaining cases, 20% of which are caused by mutations in the superoxide dismutase 1 (SOD1) gene (Lobsiger et al., 2007). In both sporadic and FALS, there can be a loss of upper and/or lower motor neurons (Cleveland and Rothstein, 2001), resulting in similar pathology (Barber and Shaw, 2010).

The G93A-SOD1 transgenic mouse, which over-expresses a mutated form of the human SOD1 gene (Achilli et al., 2005), has been studied as an experimental model for FALS. Indeed, it presents with clinical symptoms and neuropathological features that mimic those

characteristic of FALS (Achilli et al., 2005; Rosen, 1993), such as severe hind limb paralysis with atrophy of skeletal muscles (Tu et al., 1996). In G93A-SOD1 mice, atrophy of the diaphragm muscles (Holzbaur et al., 2006) results in respiratory failure and death (Tankersley et al., 2007).

It is generally accepted that ALS is caused by death of motor neurons. However, there is some uncertainty as to the sequence of motor neuron degeneration resulting in disease. Indeed, several studies in the mouse model have shown dysfunction/degeneration of the neuromuscular junction (Frey et al., 2000; Kennel et al., 1996) at times when motor neuron loss is not detected in the mice (Chiu et al.,1995). Furthermore, distal axonopathy was shown to occur early, following neuromuscular junction impairment, but before neuronal degeneration and onset of symptoms (Fischer et al., 2004). Muscle atrophy was shown to precede this sequence of events in the mouse model (Brooks et al., 2004), and recent studies in mice expressing mutant SOD1 gene variants selectively in skeletal muscle suggest that muscle degeneration might itself lead to neurodegeneration and cuse ALS (Dobrowolny et al., 2008; Dupuis and Echaniz-Laguna, 2010; Wong and Martin, 2010).

The aim of this study was to investigate further the temporal uence of neurodegeneration in relation to muscle degeneration, in G93A-SOD1 mice. For this purpose, we have used magnetic resonance imaging (MRI), a non-invasive neuroimaging tool that allows longitudinal examination of the same animal, to investigate changes in both brain and skeletal muscle at various phases of disease development and progression. We have combined MRI investigation with muscle

histological analysis and motor tests to time pathological changes in the brain versus pathological changes in muscle architecture, in relation to clinical signs.

Materials and methods

Animals

Transgenic G93A-SOD1 (B6SJL-Tg(SOD1*G93A)1Gur) mice carrying a high-copy number (approximately 27 copies) of mutant human allele SOD1, transgenic Wt-SOD1 (B6SJL-Tg(SOD1)2Gur/J) mice, and age-matched B6.SJL mice were purchased from Charles Rivers Laboratories International, Inc. (Wilmington, MA, USA), maintained and bred at the animal house of Neurological Institute Foundation “Carlo Besta,” according to the institutional guidelines and international laws (EEC Council Directive 86/609, OJL 358, 1, December 12, 1987, NIH Guide for the Care and Use of Laboratory Animals, U.S. National Research Council, 1996). The Ethics Committee of the Institute approved the study. All necessary steps were taken to ameliorate suffering to animals involved in the study. Animals were sacrificed by exposure to carbon dioxide. Male mice were used in all the studies.

Genotyping of transgenic mice

Transgenic G93A-SOD1 or Wt-SOD1 progenies were identified by real-time PCR amplification (RT-PCR) of the mutant or wild-type human SOD1 gene, respectively. DNA was extracted from tail tissue using GenElute™ mammalian Genomic DNA Miniprep kit (Sigma, St. Louis, MO, USA), according to the manufacturer's instructions.

For the quantification of SOD1 gene copy number, DNA was subjected to RTPCR as previously described (Alexander et al., 2004), with some modifications. Briefly, primers and probe for human SOD1 were forward primer, 5′-GGCCGATGTGTCTATTGAAGATT-3′; reverse primer, 5′-TGCGGCCAATGATGCA-3′; and probe, 5′-6FAM-ATCTCACTCTCAGGAGAC- MGB-3′. The standard curve was performed using serial dilutions of DNA isolated from brain of a G93A-SOD1 mouse known to have 27 copies of mutated SOD1 gene or a Wt-SOD1 mouse known to have 27 copies of wild-type SOD1 gene (parents obtained from Charles River International). RT-PCR reactions were performed in a final volume of 20 µl containing 5 ng DNA, 10 µl TaqMan Universal PCR Master mix (Applied Biosystems, Foster City, CA, USA), 300 nM forward primer, 200 nM reverse primer, and 150 nM probe. Following incubations at 50 °C for 2 min and at 95 °C for 10 min, 40 cycles of 1 s at 95 °C followed by 1 min at 60 °C were carried out in a 7500 Fast Real-Time PCR System (Applied Biosystems). The standard curve was obtained automatically through the 7500 Fast System software. Mouse IL-2 gene amplification was performed to normalize for DNA input (Alexander et al., 2004).

Determination of muscular deficit

Male G93A-SOD1 and B6.SJL control mice (n=7 per group) were evaluated at weekly intervals from week 8 to week 18 for signs of muscular deficit, according to motor function, paw grip endurance (PaGE), and body weight. Motor function and PaGE tests were performed as previously described (Weydt et al., 2003). Briefly, the

following hanging wire test was used for the PaGE test: the mouse was placed on a wire grid (wire thickness, 2 mm) that was shaken gently to prompt the mouse to hold onto the wire and the grid was turned upside down. The time taken for the mouse to let go of the grid was measured for three attempts and the mean time±SD was recorded. Impairment of motor function was scored as follows (Weydt et al., 2003): 4=moving normally; 3=obvious hind limb tremors; 2=gait abnormalities; 1=dragging of at least one hind limb; 0=inability to move.

Histological analysis

Muscle tissue was obtained from the hind limb (biceps) of three B6.SJL control and three G93A-SOD1 mice at 8, 12, 15, and 18 weeks of age, immediately embedded in Optimal Cutting Temperature compound (Bio-Optica, Milan, Italy), and stored at −80 °C until histological analysis. For each animal, four frozen tissue sections (10 μm thick) were stained with hematoxylin-eosin and examined by optical microscopy (Nikon GMBH, Germany) at 40× magnification. Muscle fiber diameters were measured using Image Pro-Plus (Media Cybernetics, Silver Spring, MD, USA). Fiber diameter was defined as the widest transversal distance. For each hind limb muscle section examined (four sections per mouse), fiber diameters were measured in ten randomly selected microscope fields.

MRI analysis

MRI experiments were performed on a 7-Tesla Bruker Biospec 70/ 30 USR scanner, horizontal bore (Bruker BioSpin, Ettlingen, Germany)

equipped with a BGA 20 (200 mT/m) gradient system. Seven male G93A-SOD1 mice and seven B6.SJL control mice were scanned for both brain and muscle MRI at age intervals that correspond to distinct disease phases: week 8 (asymptomatic phase), week 12 (clinical disease onset), week 15 (symptomatic phase), and week 18 (terminal stage), with a 3-day interval between muscle and brain MRIs to enable the animals to recover from the anesthesia. Five male G93A-SOD1 mice and five B6.SJL control mice were also scanned for brain MRI at week 10. Five male G93A-SOD1 mice and five B6.SJL control mice were analyzed for muscle MRI at week 6 to check if normal muscle mass is achieved developmentally in G93A-SOD1 mice. Three Wt-SOD1 mice were scanned for brain and muscle MRI at week 18 to ensure suitability of B6.SJL mice as controls throughout the study. Mice were anesthetized with 1.5–2% isoflurane (60:40 N2O:O2 (vol:vol), flow rate 0.8 L/min). The respiratory rate was monitored by pneumatic sensor to detect the depth of anesthesia during MRI acquisition. Mice were positioned on an animal bed equipped with a nosecone for gas anesthesia, three point-fixation system (tooth-bar and ear-plugs), and opening for throat access and body temperature stabilization.

Protocol for muscle MRI

A 35 mm quadrature volume coil was used for RF excitation and signal reception. For anatomical references, images were acquired in three orthogonal planes: axial, sagittal, and coronal. T1-weighted spin-echo images were performed using the following parameters: TE=11.7 ms, TR=454.6 ms, FOV 30×30 mm, 18 axial slices covering the entire

hind limb without gap, slice thickness=1 mm, image matrix=256×256 pixels, 10 averages, in plane resolution=117 μm. The total acquisition time was 19 min and 23 s.

Protocol for brain MRI

A 75 mm birdcage linear coil was used for RF excitation. A mouse brain surface coil was used for signal reception. T2-weighted fast spinecho images were performed using a rapid acquisition relaxation enhanced (RARE) sequence with the following parameters: TE=54 ms, TR=3500 ms, RARE factor=8, FOV 22×22 mm, 26 slices axial, sagittal, and coronal plane, slice thickness=0.60 mm, image matrix=256×256 pixels, 10 averages, in plane resolution=86 μm.
The total acquisition time was 22 min and 24 s.

Processing of MRI data

In order to quantify the total hind limb muscle volume, muscles were manually segmented from fat and bone by two independent radiologists, blinded for the health status of the animals, using the Bruker Paravision (version 5.0) software. The regions of interest (ROI) were added and multiplied by slice thickness to obtain the entire volume of the hind limb muscles for each animal.

In order to quantify the hyperintensity observed in only in hypoglossal, ambiguus, facial, and trigeminal nuclei (see Results), nuclei were manually segmented using the Bruker Paravision (version 5.0) software and the nuclei signal intensity was measured and expressed in terms of Contrast to Noise Ratio (CNR) defined as

(Nucleus-NormalTissue)/Noise, where Nucleus is the mean signal intensity of the nucleus, NormalTissue is the mean signal intensity of an adjacent ROI in the surrounding tissue at the same depth and Noise is the standard deviation of the background noise.

Statistical analysis

Statistical analysis was performed using paired and unpaired twotailed Student's t-test, and data were expressed as mean±SD; P valuesb0.05 were considered statistically significant. GraphPad Prism version 4.0 (GraphPad Software, San Diego, CA, USA) was used for data elaboration and statistical analysis.

Results

Longitudinal motor deficit analysis in G93A-SOD1 mice

The time course of disease progression in G93A-SOD1 mice was monitored by motor function scoring, PaGE, and body weight (Fig. 1). The first clinical signs of motor neuron disease in the seven male G93A-SOD1 mice were observed from week 12, as shown by motor scores indicating obvious hind limb tremor (mean score±SD=3.40± 0.10 vs. 4.00±0.00 in control mice, Pb0.01; Fig. 1) and PaGE test showing reduced muscular strength (mean grip time±SD=52.00± 3.35 s vs. 75.00±1.80 s in control mice, Pb0.001; Fig. 1). The difference in mean body weight of G93A-SOD1 mice and B6.SJL control mice was significant from week 13 (23.00±0.40 g vs. 25.00±0.53 g for control mice; Pb0.05; Fig. 1); indeed, by week 18, G93A-SOD1miceweighed on average 13 g less than B6.SJL control mice (20.00±0.40 g vs. 33±0.65 g for control mice, Pb0.001; Fig. 1).

Longitudinal quantitative MRI analysis demonstrates significant losses in muscle mass in G93A-SOD1 mice from week 8

At week 6, quantitative MRI analysis of hind limb muscle volume indicated that muscle mass in G93A-SOD1 mice did not differ significantly from that in B6.SJL control mice (1.54±0.36 cm3 vs. 1.60±0.25 cm3; Fig. 2B), indicating that normal muscle mass was achieved developmentally in the G93A-SOD1 mice. However, MRI analysis showed a significant reduction in muscular mass in G93ASOD1 mice as compared to B6.SJL control mice at week 8 (1.51± 0.08 cm3 vs. 1.74±0.04 cm3, Pb0.05; Figs. 2A and B). At week 12, while muscle mass had increased in control mice (1.94±0.07 cm3) as expected, there was a further decrease in muscle volume in G93ASOD1 mice (1.41±0.10 cm3). Henceforth, muscle volume continued to decrease in G93A-SOD1 mice (Fig. 2A), while it increased in B6.SJL control mice (week 15: 1.23±0.08 cm3 vs. 2.19±0.09 cm3, Pb0.001; week 18: 0.89±0.25 cm3 vs. 2.24±0.12 cm3, Pb0.001; Fig. 2B). As can be seen in Fig. 2, there was no difference in muscle volume as late as week 18 in Wt-SOD1 control mice (2.39±0.21 cm3), as compared to B6.SJL control mice (2.24±0.12 cm3), indicating that expression of the human wild-type SOD1 transgene has no deleterious effect on the muscle in these mice, in contrast to that of the mutated G93A-SOD1 gene, and that B6.SJL mice are indeed adequate controls for this study.

Longitudinal histological analysis shows increasing derangement of muscle architecture in G93A-SOD1 mice from week 8

We observed a reduction in muscle fiber diameter in G93A-SOD1 mice compared to B6.SJL control mice from as early as week 8, when the animals were still asymptomatic (Fig. 3A). As disease progressed from weeks 12 to 18, muscle organization in G93A-SOD1 miceappeared increasingly altered, with numerous, large endomysial spaces within the fibers and a majority of fibers with highly reduced diameter; as an additional evidence of muscle atrophy, regenerating fibers with centrally located nuclei and small diameter were present at week 18 (Fig. 3A). Measurement of fiber diameter in G93A-SOD1 mice, as compared to B6.SJL control mice, indicated that the reductions observedwere significant fromweek 8 (259.65±18.08 μmvs. 317.00±60.82 μm, Pb0.005; Fig. 3B). Further highly significant decreases in muscle fiber diameter occurred as disease progressed in the G93ASOD1 mice (37.86±12.42 μm at week 18 vs. 259.65±18.08 μm at week 8, Pb0.001; Fig. 3B).

Longitudinal brain MRI analysis shows neurodegeneration in G93ASOD1 mice from week 10

When MRI analysis of the whole brain was carried out at regular intervals from weeks 8 to 18, clear T2-weighted MRI hyperintensity, indicative of neurodegeneration, was detected in G93A-SOD1 mice from week 10 (Fig. 4A). These hyperintensity signals were observed only in the brainstem at areas corresponding to the trigeminal, facial, ambiguus, and hypoglossal motor nuclei from which originate secondary motor neurons (Fig. 4A). No significant signals were

observed in these mice at week 8 (Figs. 4A and B), when muscular mass and muscle fiber diameter are significantly reduced (Figs. 2 and 3). These hyperintensive signals increased as disease progressed indicating an increase in motor neuron degeneration (Figs. 4A and B). Thus, while signals remained at baseline in nuclei of control brain throughout the study period (trigeminal: 1.11±0.40 and 1.15±0.25; facial: 1.42±0.55 and 0.82±0.11; ambiguus: 0.89±0.29 and 0.59± 0.29; and hypoglossal: 4.26±1.65 and 7.69±0.81, at weeks 8 and 18, respectively. Fig. 4B), hyperintensity in the nuclei increased steadily in G93A-SOD1 mice (trigeminal: 2.16±0.75 and 8.55±1.10; facial: 2.24±0.75 and 10.72±1.25; ambiguus: 0.97±0.88 and 4.01±0.61; and hypoglossal: 6.05±1.9 and 18.62±1.25, at weeks 8 and 18, respectively. Fig. 4B). Evidence of neurodegeneration was significant from week 10 in trigeminal, facial, and ambiguus nuclei, and from week 15 in the hypoglossal nucleus (Fig. 4). We did not detect any significant hyperintensive signal in these mice in the motor cortex where first motor neurons originate. It should be noted that hyperintensity was not detected in the brain of Wt-SOD1 control mice as late as week 18 (Supplemental Figure), indicating that these mice do not differ from B6. SJL control mice also in this respect; these data confirm that B6.SJL miceare also adequate controls for brain MRI comparison with G93A-SOD1 mice.

Discussion

Our aim in this study was to establish unequivocally the sequence of muscular versus neurological events leading to disease in the G93ASOD1 mouse model of ALS. We have addressed this aim

through longitudinal MRI studies of both skeletal muscle and brain starting at week 8, that is from about 4 weeks before clinical onset, and evaluated the data in parallel with muscle histology and motor function.

MRI has been used experimentally in ALS to investigate CNS alterations at the final phase of the disease, that is at the symptomatic stage in patients (Charil et al., 2009) and at week 18 in SOD1G93A G1H transgenic mice (Andjus et al., 2009). In the mouse model, MRI study of the brain from the frontal cortex through the brainstem medulla at week 18 revealed hyperintensity signals in the brainstem at the ambiguus and trigeminal motor nuclei (Andjus et al., 2009), similar to what we have observed from week 10 in G93A-SOD1 mice in the present study. In a previous longitudinal MRI study of hind limb muscle in G93A-SOD1 mice, Brooks et al. observed significant decrease in muscle volume of mutant male mice from 8 weeks of age (Brooks et al., 2004), as we have also observed. Indeed, our analysis of T1-weighted images of hind limb muscle showed a significant reduction as early as week 8 in muscle volume of G93ASOD1 mice, as compared to control mice. These data indicate that, while early clinical signs first appear around week 12 in G93A-SOD1 mice (Weydt et al., 2003), as we confirm through concomitant three way monitoring of clinical disease progression from week 8, disease onset actually occurs in these mice at least 4 weeks earlier. Our longitudinal histological analysis confirms these MRI findings; indeed, evidence of muscle atrophy with significant reductions in muscle fiber diameter was observed from week 8 onwards in the G93A-SOD1 mice. Increasing muscle atrophy was commensurate with worsening clinical

signs. Thus, endomysial spaces were observed among muscle fibers at week 12, when G93A-SOD1 mice presented with early signs of motor impairment; at weeks 15 and 18, when mice were highly impaired in their muscle function, the muscles presented with large numbers of fibers with highly reduced diameter, large endomysial spaces, and some evidence of regenerating fibers, all of which are highly representative of muscular atrophy in this murine ALS model (Zhang et al., 2008) and in other motor diseases (Dupuis and Echaniz-Laguna, 2010).

Our concomitant longitudinal MRI analysis of the whole brain demonstrated unequivocally that muscular degeneration in G93ASOD1 mice occurs prior to neurodegeneration. Indeed, clear T2-weighted MRI hyperintensity was only detected at week 10, whereas significant alterations were observed in the muscle at week 8. These results corroborate data obtained in a previous longitudinal study of brain changes by MRI analysis, where T2 values were significantly higher for the three hypoglossal, trigeminal and facial brainstem nuclei analyzed from day 80 after birth (Bucher et al., 2007). In that study, morphological alterations in the three brainstem nuclei investigated were observed by histological analysis around the same time point, i.e., 80 days after birth, when changes in the MRI images became obvious (Bucher et al., 2007). Recent studies with transgenic mice expressing the mutated human G93A-SOD1 gene exclusively in skeletal muscle have demonstrated that skeletal muscle-restricted expression of the mutant SOD1G93A gene leads to muscle atrophy and dysfunction in these mice (Dobrowolny et al., 2008; Wong and Martin, 2010). Most importantly,Wong and Martin showed that such

skeletal muscle-restricted expression of this mutated gene is sufficient to also cause dismantled neuromuscular junction and motor neuron distal axonopathy resulting in motor neuron disease in these mice, suggesting that subclinical disease in skeletal muscle can be an initiating causal pathologic process rather than the consequence of neurogenic atrophy (Wong and Martin, 2010). It is noteworthy that these effects were observed at low levels of expression of the mutated gene (Dobrowolny et al., 2008; Wong and Martin, 2010) and indeed, partial (60%) siRNA-mediated suppression of mutant SOD1 in muscle of SOD1-G93A mice did not affect disease in these mice (Miller et al., 2006). Our longitudinal study demonstrating clear muscular alterations before any evidence of neurodegeneration and clinical signs in this ALS murine model fully supports the conclusion of Wong and Martin that muscle fiber degeneration could lead to neuronal damage (Wong and Martin, 2010). Most interestingly, our 7T-MRI analysis demonstrated that, in the brain of G93A-SOD1 mice, the secondary motor neurons originating in the brainstem, and not the first motor neurons, are the first affected by the neurodegenerative process. Similar MRI findings were obtained, for the end stage of the disease, in ALS rats expressing the same mutated (G93A) human SOD1 gene (Andjus et al., 2009) and in other mouse models (Zang et al., 2004). In a recent study, however, Özdinler et al. (2011) observed degeneration of upper motor neurons in their hSOD1G93A transgenic mice, as early as at postnatal day 30. While these findings seemingly contradict our data, it should be noted that there are significant differences that could account for this discrepancy. The hSOD1G93A mice used in the study of Özdinler et al. differ significantly from the

mice we have studied here: they are on a genetic C57Bl/6J background, whereas the mice in the present study are on a mixed C57Bl/6J x SJL background, and they apparently have a much earlier disease onset. Indeed, according to the authors, their hSOD1G93A mice are already symptomatic at postnatal day 50, albeit disease course was not shown, whereas the G93A-SOD1 mice we have studied have a disease onset around 30 days later at week 12, as was also shown by other studies (Tu et al., 1996; Tankersley et al., 2007). Accordingly, it is highly possible that other manifestations of the disease, including muscle degeneration, occur earlier in these mice also. However, because muscle degeneration was not studied by Özdinler et al., it is not possible to ascertain whether or not their findings could affect our conclusions. At present, therefore, our findings further corroborate the postulate that in the murine model of ALS, neurodegeneration resulting from muscular degeneration occurs through a retrograde “dying-back” mechanism (Wong and Martin, 2010).

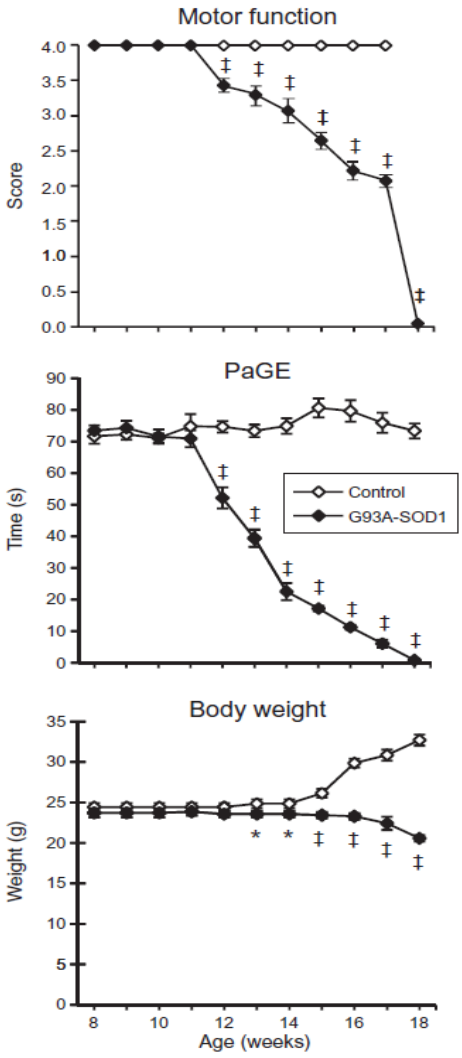

Fig. 1. Longitudinal analysis of motor deficit in G93A-SOD1 mice. G93A-SOD1 and control B6.SJL mice (n=7 per group) were monitored weekly as described in Materials and methods for motor function, PaGE, and body weight, from weeks 8 to 18 after birth. Data are presented as mean±SD. *Pb0.05; ‡Pb0.001

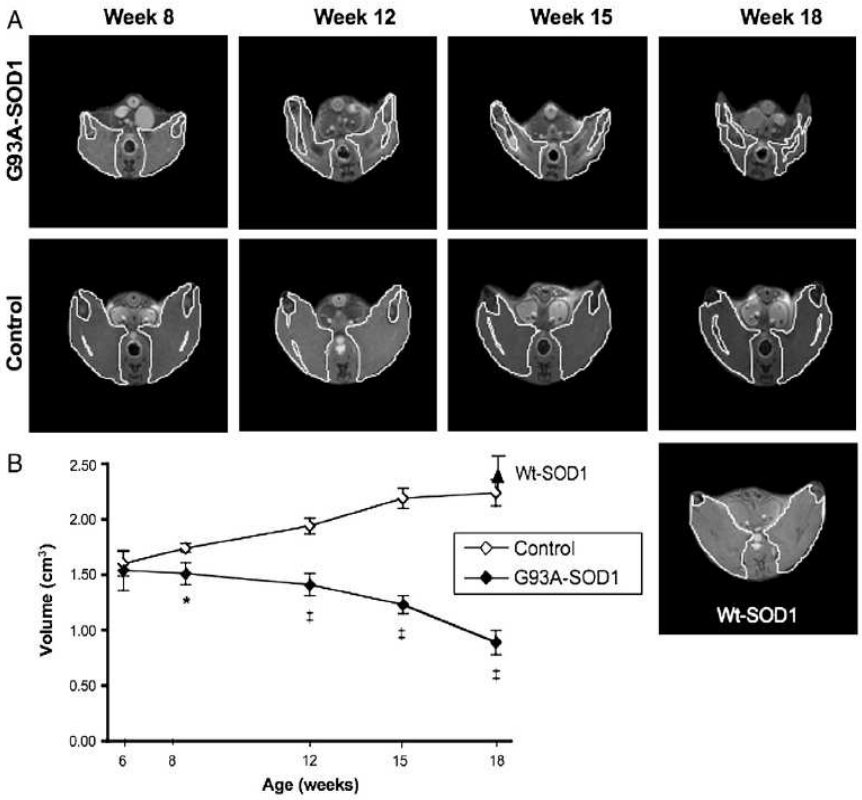

Fig. 2. Longitudinal MRI analysis of hind limb muscle in G93A-SOD1 mice. Representative T1-weighted MR images of axial slices through the hind limb of G93A-SOD1 and B6.SJL control mice from weeks 8 to 18. ROI are indicated by white outline. B. ROI quantification of hind limb muscle volume in G93A-SOD1 and control B6.SJL mice from weeks 6 (n=5 per group) to 18 (n=7 per group from week 8). Data are presented as mean±SD. *Pb0.005; ‡Pb0.001. A representative MR image of hind limb Wt-SOD1 muscle taken at week 18 is also presented in A, and the mean muscle mass for three Wt-SOD1 mice at week 18 is shown in B.

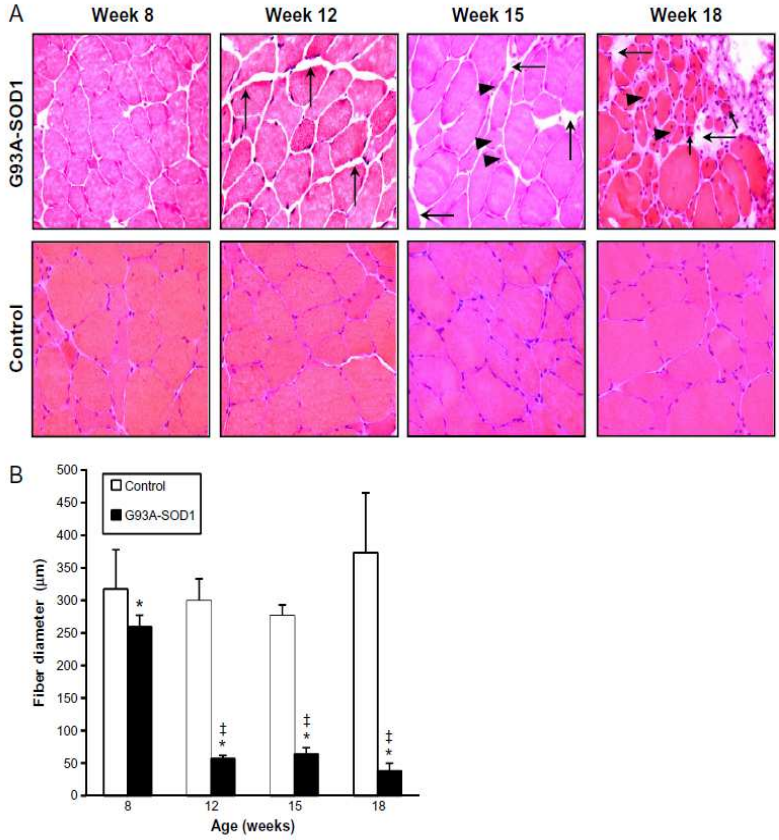

Fig. 3. Longitudinal histological analysis of hind limb muscle in G93A-SOD1 mice. Representative transversal hind limb muscle sections in G93A-SOD1 and control B6.SJL mice stained with hematoxylin/eosin. Long arrows indicate endomysial spaces; arrowheads indicate fibers with reduced diameter; and short arrows indicate fibers with centrally located nuclei indicative of fiber regeneration. Magnification 40×. B. Measurement of fiber diameter in hind limb muscle of G93A-SOD1 and control B6.SJL mice from weeks 8 to 18. Each histogram represents the mean diameter±SD of muscle fibers measured in four hind limb muscle sections from three mice in each group. *Pb0.005 vs. control at each time point; ‡Pb0.001 for G93A-SOD1 mice at indicated times vs. week 8.

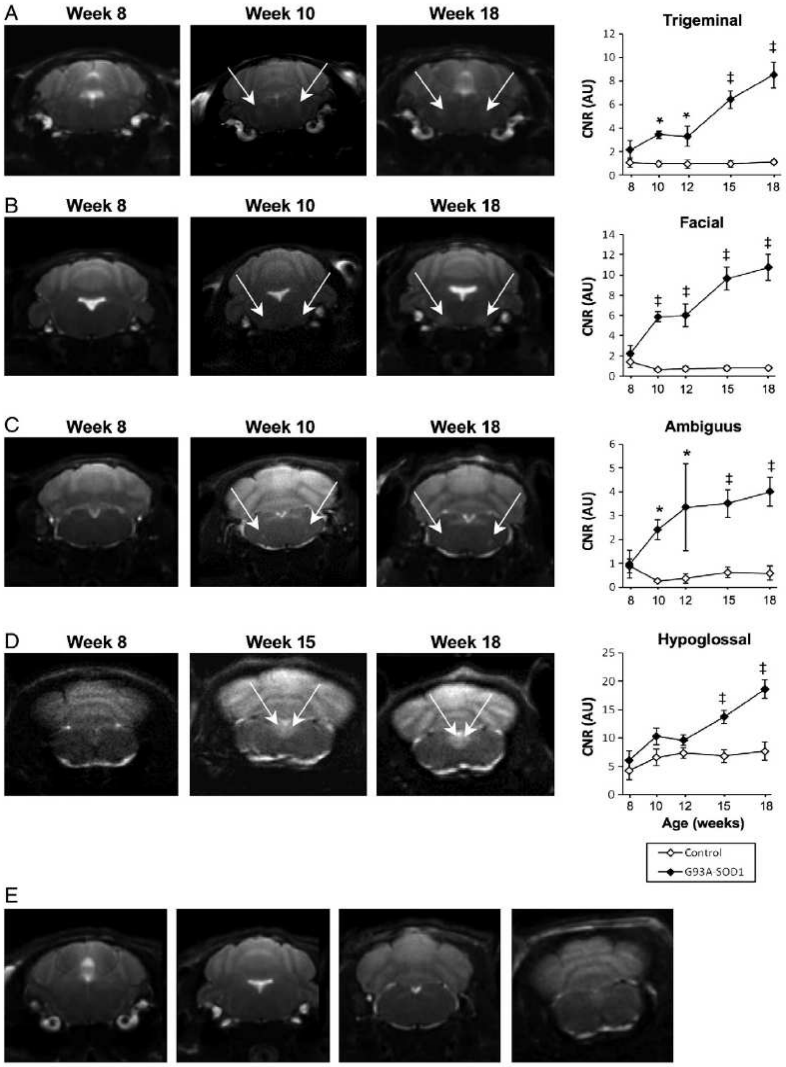

Fig. 4. Longitudinal MRI analysis of brain in G93A-SOD1 mice.

A–D. Representative T2-weighted MR images of trigeminal, facial, and ambiguus nuclei at week 8, week 10 when degeneration first appeared, and week 18 (A-C), and of hypoglossal nucleus at week 8, week 15 when degeneration first appeared, and week 18 (D), in G93A-SOD1 mice. The righthand graphs show the quantification of

hyperintensity signals in the respective brainstem motor nuclei in G93A-SOD1 and B6.SJL control mice (n=7 per group) from weeks 8 to 18.Data are presented as mean±SD. *Pb0.005 and ‡Pb0.001 vs. control at relevant time points. E. Representative T2-weighted MR images of brainstem areas of trigeminal, facial, ambiguus, and hypoglossal nuclei in B6.SJL control mice (week 18).

References

Achilli, F., Boyle, S., Kieran, D., Chia, R., Hafezparast, M., Martin, J.E., Schiavo, G., Greensmith, L., Bickmore, W., Fisher, E.M., 2005. The SOD1 transgene in the G93A mouse model of amyotrophic lateral sclerosis lies on distal mouse chromosome 12. Amyotroph. Lateral Scler. Other Motor Neuron Disord. 6, 111–114.

Alexander, G.M., Erwin, K.L., Byers, N., Deitch, J.S., Augelli, B.J., Blankenhorn, E.P., Heiman-Patterson, T.D., 2004. Effect of transgene copy number on survival in the G93A SOD1 transgenic mouse model of ALS. Brain Res. Mol. Brain Res. 130, 7–15.

Andjus, P.R., Bataveljić, D., Vanhoutte, G., Mitrecic, D., Pizzolante, F., Djogo, N., Nicaise, C., Gankam Kengne, F., Gangitano, C., Michetti, F., van der Linden, A., Pochet, R., Bacić, G., 2009. In vivo morphological changes in animal models of amyotrophic lateral sclerosis and Alzheimer's-like disease: MRI approach. Anat. Rec. (Hoboken) 292, 1882–1892.

Barber, S.C., Shaw, P.J., 2010. Oxidative stress in ALS: key role in motor neuron injury and therapeutic target. Free Radic. Biol. Med. 48, 629–641.

Brooks, K.J., Hill, M.D., Hockings, P.D., Reid, D.G., 2004. MRI detects early hindlimb muscle atrophy in Gly93Ala superoxide dismutase-1 (G93A SOD1) transgenic mice, an animal model of familial amyotrophic lateral sclerosis. NMR Biomed. 17, 28–32.

Bucher, S., Braunstein, K.E., Niessen, H.G., Kaulisch, T., Neumaier, M., Boeckers, T.M., Stiller, D., Ludolph, A.C., 2007. Vacuolization correlates with spin-spin relaxation time in motor brainstem nuclei

and behavioural tests in the transgenic G93A-SOD1 mouse model of ALS. Eur. J. Neurosci. 26, 95–101.

Charil, A., Corbo, M., Filippi, M., Kesavadas, C., Agosta, F., Munerati, E., Gambini, A., Comi,

G., Scotti, G., Falini, A., 2009. Structural and metabolic changes in the brain of patients with upper motor neuron disorders: a multiparametric MRI study. Amyotroph. Lateral Scler. 10, 269–279.

Chiu, A.Y., Zhai, P., Dal Canto, M.C., Peters, T.M., Kwon, Y.W., Prattis, S.M., Gurney, M.E., 1995. Age-dependent penetrance of disease in a transgenic mouse model of familial amyotrophic lateral sclerosis. Mol. Cell. Neurosci. 6, 349–362.

Cleveland, D.W., Rothstein, J.D., 2001. From Charcot to Lou Gehrig: deciphering selective motor neuron death in ALS. Nat. Rev. Neurosci. 2, 806–819.

Dobrowolny, G., Aucello, M., Rizzuto, E., Beccafico, S., Mammucari, C., Boncompagni, S., Bonconpagni, S., Belia, S., Wannenes, F., Nicoletti, C., Del Prete, Z., Rosenthal, N., Molinaro, M., Protasi, F., Fanò, G., Sandri, M., Musarò, A., 2008. Skeletal muscle is a primary target of SOD1G93A-mediated toxicity. Cell Metab. 8, 425–436.

Dupuis, L., Echaniz-Laguna, A., 2010. Skeletal muscle in motor neuron diseases: therapeutic target and delivery route for potential treatments. Curr. Drug Targets 11, 1250–1261.

Fischer, L.R., Culver, D.G., Tennant, P., Davis, A.A., Wang, M., Castellano-Sanchez, A., Khan, J., Polak, M.A., Glass, J.D., 2004. Amyotrophic lateral sclerosis is a distal axonopathy: evidence in mice and man. Exp. Neurol. 185, 232–240.

Frey, D., Schneider, C., Xu, L., Borg, J., Spooren, W., Caroni, P., 2000. Early and selective loss of neuromuscular synapse subtypes with low sprouting competence in motoneuron diseases. J. Neurosci. 20, 2534–2542.

Holzbaur, E.L.F., Howland, D.S.,Weber, N., Wallace, K., She, Y., Kwak, S., Tchistiakova, L.A., Murphy, E., Hinson, J., Karim, R., Tan, Y.X., Kelley, P., McGill, C.K.,Williams, G., Hobbs, C., Doherty, P., Zaleska, M.M., Pangalos, M.N., Walsh, F.S., 2006. Myostatin inhibition slows muscle atrophy in rodent models of amyotrophic lateral sclerosis. Neurobiol. Dis. 23, 697–707.

Kennel, P.F., Finiels, F., Revah, F., Mallet, J., 1996. Neuromuscular function impairment is not caused by motor neurone loss in FALS mice: an electromyographic study. Neuroreport 7, 1427–1431.

Lobsiger, C.S., Boillée, S., Cleveland, D.W., 2007. Toxicity from different SOD1 mutants dysregulates the complement system and the neuronal regenerative response in ALS motor neurons. Proc. Natl. Acad. Sci. U. S. A. 104, 7319–7326.

Miller, T.M., Kim, S.H., Yamanaka, K., Hester, M., Umapathi, P., Arnson, H., Rizo, L., Mendell, J.R., Gage, F.H., Cleveland, D.W., Kaspar, B.K., 2006. Gene transfer demonstrates that muscle is not a primary target for non-cell-autonomous toxicity in familial amyotrophic lateral sclerosis. Proc. Natl. Acad. Sci. U. S. A. 103, 19546–19551.

Özdinler, P.H., Benn, S., Yamamoto, T.H., Güzel, M., Brown, R.H., Macklis, J.D., 2011. Corticospinal motor neurons and related subcerebral projection neurons undergo early and specific

neurodegeneration in hSOD1G93A transgenic ALS mice. J. Neurosci. 31, 4166–4177.

Rosen, D.R., 1993. Mutations in Cu/Zn superoxide dismutase gene are associated with familial amyotrophic lateral sclerosis. Nature 364, 362.

Tankersley, C.G., Haenggeli, C., Rothstein, J.D., 2007. Respiratory impairment in a mouse model of amyotrophic lateral sclerosis. J. Appl. Physiol. 102, 926–932.

Tu, P.H., Raju, P., Robinson, K.A., Gurney, M.E., Trojanowski, J.Q., Lee, V.M., 1996. Transgenic mice carrying a human mutant superoxide dismutase transgene develop neuronal cytoskeletal pathology resembling human amyotrophic lateral sclerosis lesions. Proc. Natl. Acad. Sci. U. S. A. 93, 3155–3160.

Weydt, P., Hong, S.Y., Kliot, M., Möller, T., 2003. Assessing disease onset and progression in the SOD1 mouse model of ALS. Neuroreport 14, 1051–1054.

Wong, M., Martin, L.J., 2010. Skeletal muscle-restricted expression of human SOD1 causes motor neuron degeneration in transgenic mice. Hum. Mol. Genet. 19, 2284–2302.

Zang, D.W., Yang, Q., Wang, H.X., Egan, G., Lopes, E.C., Cheema, S.S., 2004. Magnetic resonance imaging reveals neuronal degeneration in the brainstem of the superoxide dismutase 1 transgenic mouse model of amyotrophic lateral sclerosis. Eur. J. Neurosci. 20, 1745–1751.

Zhang, J., Zhang, G., Morrison, B., Mori, S., Sheikh, K.A., 2008. Magnetic resonance imaging of mouse skeletal muscle to measure denervation atrophy. Exp. Neurol. 212, 448–457

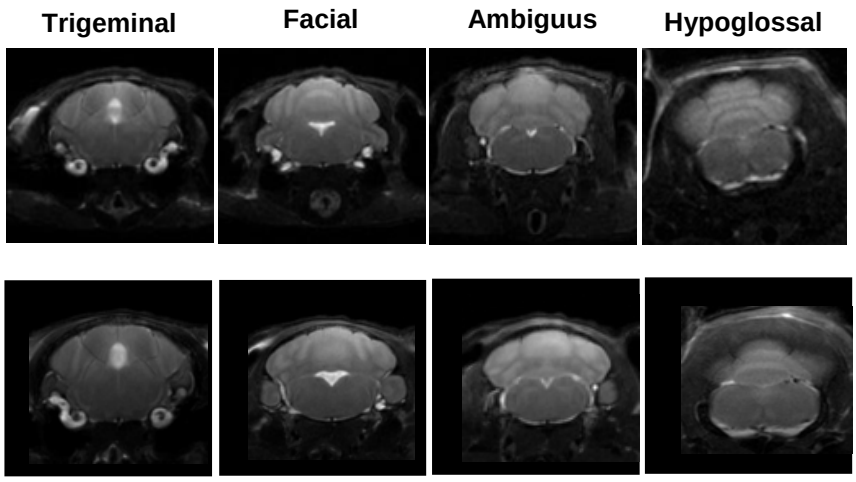

Supplemental figure. MR images of brainstem nuclei areas in control B6.SJL and Wt-SOD1 mice at week 18. Brain MRI analysis in B6.SJL (upper panel) and Wt-SOD1 (lower panel) mice shows the absence of hyperintensity indicative of neurodegeneration in both control groups as late as at week 18, thereby confirming the suitability of B6.SJL mice as controls in this study.

CHAPTER 3

Altered miRNA expression skews neural fate in G93A ependymal stem progenitors.

Stefania Marcuzzo, Nicole Kerlero de Rosbo, Fulvio Baggi, Silvia Bonanno, Claudia Barzago, Paola Cavalcante, Dimos Kapetis, Margherita Bodini, Renato Mantegazza, and Pia Bernasconi.

Submitted Stem Cells and Development

Abstract

Amyotrophic lateral sclerosis (ALS) is a fatal disorder characterized by motor neuron degeneration.

To examine why de novo neurogenesis fails in ALS, we investigated spinal cord and cultures of spinal cord ependymal stem/progenitor cells (epSPCs) isolated from G93A-SOD1 mice at 8(asymptomatic) and 18 (advanced disease) weeks.

We characterized the ability of epSPC cultures to proliferate and differentiate into the three neural cell lineages. We used immunocytochemistry to characterise cell types. We used real-time PCR to assess miR-9, miR-124a, miR-19a and miR-19b expression.

Cultured G93A-SOD1 epSPCs produced neurospheres of self-renewing cells that differentiated into the three neural cell lineages, but there were more neurons and fewer astrocytes than controls; neurons were small and astrocytes were activated. miR-9 and miR-124a were upregulated in differentiating G93A-SOD1 epSPCs, particularly those taken at 18 weeks, but were downregulated in the most severely affected spinal cord regions. miR-19a and miR-19b expression was altered in G93A-SOD1 spinal cord and during G93A-

SOD1 epSPC differentiation. Although neural stem progenitor cells (nestin-positive) were abundant, few neuroblasts (Dlx2-positive) were present in G93A-SOD1 spinal cord.

Our findings link lack of neurogenesis in the spinal cord of G93A-SOD1 mice to defective expression miRNAs involved in neuronal differentiation and cell-cycle regulation. Furthermore, since G93A-SOD1 epSPCs seem to retain a memory (altered neural fate programming) of dysregulated spinal cord, they could be useful as an in vitro model for investigating ALS pathogenesis and new therapeutic agents.

Introduction

Amyotrophic lateral sclerosis (ALS) is a fatal progressive disorder in which motor neurons of cortex, brainstem, and spinal cord degenerate. About 90% of ALS cases are sporadic (SALS) and most of these are of unknown aetiology. Familial ALS (FALS) makes up the remaining cases, 12- 23% of which are caused by mutations in the superoxide dismutase 1 (SOD1) gene [1]. The SALS and FALS forms are clinically indistinguishable [2] and increasing evidence indicates that genetic factors are also involved in SALS [1].

The G93A-SOD1 transgenic mouse, a widely used ALS animal model over-expressing the G93A mutated human SOD1 gene, has symptoms and neuropathological features resembling those of human ALS, [3] including severe hind limb paralysis and skeletal muscle atrophy starting from postnatal week (wk) 8 [4].

No current treatment can prevent or reduce motor neuron degeneration in ALS, so enhancing de novo neurogenesis may be one way of

mitigating the effects of ALS [5]. Neural stem cells (NSCs) are present in the CNS of adult humans and mice, and neurogenesis occurs in both [6,7]. Several physiological and pathological conditions, including spinal cord injury and neurodegenerative diseases, promote adult neurogenesis [8,9]. And although it is unclear whether neurogenesis occurs in ALS, neural progenitor cells from post-mortem spinal cord of SALS and FALS patients have been shown to differentiate in vitro into the three neural cell lineages [10]. In ALS mice, neurodegeneration promotes the proliferation and migration of NSCs present (and normally quiescent) in spinal cord [8]. However, as in human ALS, new mature motor neurons are not generated in G93A-SOD1 mouse spinal cord [8] and it is unclear why final maturation fails.

MicroRNAs (miRNAs) are non-coding, 18-25 nucleotide-long transcripts that regulate gene expression through post-transcriptional inhibition or degradation of complementary Mrna sequences [11]. They play crucial roles in the maintenance, differentiation, and lineage commitment of embryonic and adult stem cells [12−18]. Altered miRNA expression is associated with neurodegenerative and other diseases [19−21]. Mutations in TDP-43 – a protein required for miRNA biogenesis – are associated with ALS [1], suggesting that miRNA dysfunction is involved in ALS pathogenesis. Deficiency in a skeletal muscle-specific miRNA is known to accelerate disease progression in ALS mice [22]. The transcriptional repression of motor neuron transcriptomes in SALS [23] and a cellular model of FALS [24] probably reflects altered miRNA expression. Similar

transcriptional repression has been observed in late-stage disease in G93ASOD1 mice [25].

miR-124a is expressed in neuronal cells and promotes the differentiation of neuronal progenitors into mature neurons [14,26,27]. miR-124a is expressed in microglia where it is involved in maintaining the quiescent microglial phenotype in normal CNS [28]. miR-9 is expressed specifically in neurogenic regions of the brain during development and adulthood; it promotes neurogenesis by downregulating suppressors of neuronal differentiation [29] and is upregulated during NSC differentiation [30]. Both miR-124 and miR-9 strongly influence NSC fate: their early overexpression in neural progenitors reduces the number of astrocytes in differentiated cultures, while inhibition of miR-9 alone or in combination with miR-124 reduces the number of neurons [13].

miR-19a and miR-19b are encoded by the miR-17-92 cluster linked to tumorigenesis [31], but more generally tend to target gene products involved in cell-cycle regulation. They are enriched in several stem cell types and are part of the early commitment signature marking the conserved stemto- progenitor transition [12,32].

We report here our investigations (a) of the ability of ependymal stem progenitor cells (epSPCs) from G93A-SOD1 spinal cord to differentiate into neurons, astrocytes and oligodendrocytes; (b) the expression of miR-9, miR124a, miR-19a and miR-19b in G93A-SOD1 spinal cord, and their effects on neuronal fate both in spinal cord and cultured epSPCs. Our aim was to gain insights into why motor neuron regeneration fails in ALS.

Materials and Methods

All reagents are detailed in Supplementary Table S1.

Animals

Transgenic G93A-SOD1 (B6SJL-Tg(SOD1*G93A)1Gur) and wild-type (WT)-SOD1 (B6SJLTg(SOD1)2Gur/J) mice, and B6.SJL mice were from Charles Rivers Laboratories International, Inc. (Wilmington, MA), and maintained and bred in the animal house of the Besta Institute, in accordance with the ethically approved institutional guidelines that are in compliance with national and international laws and policies (European Economic Community Council Directive 86/609, Official Journal L 358, 1, December 12, 1987; Guide for the Care and Use of Laboratory Animals, U.S. National Research Council, 1996). G93A- and WT-SOD1 progenies were identified by RT-PCR of the human SOD1 gene, as described [4]. Animals were killed, at either 8 or 18 wks of age, by exposure to carbon dioxide. Male mice were used in all studies.

Spinal cord stem/progenitor cell isolation and culture epSPCs were isolated from whole spinal cord of 8- or 18-wk-old G93A-SOD1, WT-SOD1 and B6.SJL animals. After removal of the overlaying meninges and blood vessels, spinal cord was cut into small pieces, dissociated with 0.05% collagenase I for 15 minutes at 37°C, and then processed to produce epSPC neurospheres as described [33,34], with the difference that neurospheres were usually dissociated into single cells every 7 days with 0.1% collagenase and re-plated at a lower density; expansion continued for up to 50 days to obtain sufficient cells for

further analyses and ensure that cultures were devoid of cells not forming neurospheres. The neurospheres were checked periodically by optical microscopy (Eclipse TE 2000-S, Nikon, Tokyo, Japan) and characterized for nestin expression by immunocytochemistry. Cell viability of collagenase-dissociated neurospheres was assessed by Trypan blue exclusion method.

Differentiation of epSPCs

Neurospheres in culture for 50 days were dissociated into single cells and plated onto eight Matrigel-treated 19-mm glass coverslips (7x104 cells/ml). After two days, the proliferation medium was replaced by differentiating medium, which differs for the addition of 2% fetal bovine serum and absence of growth factors. The differentiated cells were used for experiments after being in culture for 25 days, by which time the cultures had become confluent. Six separate differentiation experiments were performed for each mouse strain and subsequent experiments were performed on each of the six batches.

Immunocytochemistry

To immunostain neurospheres with nestin, they were plated onto Matrigel-treated glass coverslips, left to adhere for 3-5 hours, fixed in 4% paraformaldehyde at room temperature for 20 minutes, permeabilized with 0.1% Triton X-100, and treated with 10% normal goat serum in PBS to block non-specific binding. They were then incubated with mouse anti-nestin antibody. Immunopositivity was revealed with Cy3-conjugated goat anti-mouse IgG. Differentiated epSPCs were immunostained on Matrigel-treated coverslips as

described for neurospheres. They were reacted with the following primary antibodies: rabbit anti- NeuN antibody; mouse anti-glial fibrillary acidic protein (GFAP) antibody; mouse anti-O4 antibody; mouse anti-N-methyl-D-aspartate (NMDA) receptor 2A/B antibody; mouse anti-synaptophysin antibody. Secondary antibodies were Cy2-conjugated goat anti-mouse IgG, Cy3-conjugated goat anti-rabbit IgG, or Cy3-conjugated goat anti-mouse IgM. Neurospheres or differentiated cells were counterstained with DAPI. The coverslips were mounted with FluorSave. Confocal fluorescence images were obtained with a laser-scanning microscope (Eclipse TE 2000-E, Nikon) and analyzed with the EZ-C1 3.70 imaging software (Nikon).

Analysis and quantification of cell fate in differentiated epSPC cultures

β-tubulin-III-positive (neurons), GFAP-positive (astrocytes) and O4-positive (oligodendrocytes) cells were quantitated on 10 randomly selected fields for each coverslip. Eight coverslips were analyzed for each of the six cultures for each mouse strain. The percentages of neurons, astrocytes, and oligodendrocytes were calculated in relation to the total number of DAPI-positive cells/field, and expressed as means ± SD for each of the six cultures obtained from each mouse strain. GFAP staining intensity was measured using the Image Pro-Plus software (Media Cybernetics, Silver Spring, MD). Neuronal cell body perimeter was also measured with Image Pro-Plus on differentiated cells immunostained for synaptophysin and NMDA receptor 2A/B.

Immunohistochemistry

Lumbar spinal cord (L1-L5) was dissected out, immediately embedded in Optimal Cutting Temperature compound, and stored at -80˚C pending histological analysis. Twenty 30-Tm-thick cryostat sections were fixed in 4% paraformaldehyde, treated with 0.1% Triton X-100, incubated with 10% normal goat serum or 5% bovine serum albumin and overnight with mouse anti-nestin antibody to mark neural stem cells, mouse anti-distal-less homeobox 2 (Dlx2) antibody to mark neuronal precursors, and mouse anti-β-tubulin III antibody to mark neurons. After washing, the samples were incubated with secondary antibody: either Cy2-conjugated goat anti-mouse IgG antibody or Cy2-conjugated donkey anti-goat IgG antibody. After rinsing three times with PBS, preparations were mounted with FluorSave Reagent and images captured in a fluorescence microscope (Nikon). Negative control sections were incubated with isotype-specific non-immune immunoglobulin G (IgG) or normal goat serum. Nestin-positive cells in the ependymal zone of lumbar spinal cord were quantitated at x10 magnification on a constant 35 mm2 area, using Image Pro Plus.

Real-time PCR

A was extracted with TRIzol from 1-2x106 undifferentiated and differentiated epSPCs or 35-50 mg (wet weight) spinal cord. RNA quality was checked using a 2100Nano Bioanalyzer (Agilent Technologies, Waldbron, Germany). Total RNA was retrotranscribed using a TaqMan MicroRNA Reverse Transcription Kit with primers specific for miR-9, miR-124a, miR-19a, miR-19b, and miR-24 as

control. cDNA (corresponding to 15 ng total RNA) was amplified by quantitative real-time PCR, in triplicate, using Universal PCR master mix and pre-designed TaqMan MicroRNA assays, as indicated above, on Applied Biosystems PRIMS 7700HT Fast Real- Time PCR System. Relative miRNA expression was calculated as fold changes using the 2-UCt method with normalization against miR-24.

miRNA target prediction

Functional annotation of validated miRNA targets was performed using the Cytoscape software version 2.8.2 (http://www.cytoscape.org/) with the ClueGO plugin [35] through metabolic pathways (KEGG, Biocarta) and Gene Ontology Biological Process terms. ClueGO displays the functional terms as nodes and the relationships between the terms based on the similarity of their associated genes as edges. The degree of connectivity between terms is calculated through Cohen's kappa statistics using a threshold cutoff > 0.4. GO term fusion was applied for redundancy reduction.

Statistical analysis

Quantitative data are expressed as mean ± standard deviation (SD) of the mean. One- and 2-way analysis of variance (ANOVA) with Bonferroni post hoc test were performed to assess the significance of differences; $p < 0.05$ was considered statistically significant. GraphPad PRISM version 5.0 (GraphPad Software, San Diego, CA) was used for data elaboration and statistical analysis.

Results

Nestin-positive (stem) cells are more numerous in ependymal zone of G93A-SOD1 mouse spinal cord at 18 weeks than 8 weeks.

We first evaluated the neuroregenerative potential of G93A-SOD1 spinal cord following motor neuron degeneration by determining the expression of nestin (marker of NSCs) in the dorsal horn, ependymal zone and ventral horn of lumbar spinal cord (Fig. 1A). At postnatal wk 8, we observed fewer nestin-positive cells in and around the ependymal zone of G93A-SOD1 mice (mean ± SD =82.7 ± 16.8) than controls (mean ± SD = 118.3 ± 29.7 for B6.SJL and 110.9 ± 30.8 for WT-SOD1, $p<0.001$ and <0.05, respectively; Fig. 1B). However, at wk 18, while in B6.SJL and WT-SOD1 mice the number of nestin-positive cells in the ependymal zone remained substantially unchanged (mean ± SD = 110.9 ± 36.7 in B6.SJL and 128.3 ± 38.2 in WT-SOD1, $p>0.05$; Fig. 1B), in G93ASOD1 mice nestin-positive cell number was markedly increased (mean ± SD = 217.6 ± 43.2, compared to 8 wk and age-matched controls, $p<0.001$; Fig. 1B). We further characterized the neuroregenerative process in G93A-SOD1 lumbar spinal cord at wk 18 by staining tissue sections with antibodies against Dlx2 and β-tubulin III, markers of neuroblasts and neurons, respectively. As shown in Supplementary Fig. 1, few Dlx2- and β-tubulin III-positive cells were present in G93ASOD1mice and in controls.

Proliferation potential of epSPCs is maintained in G93A-SOD1 mice.
We next evaluated the ability of isolated epSPCs to proliferate in vitro and differentiate into the three neural lineages. epSPCs expanded slowly regardless of source (B6.SJL, WT-SOD1, G93ASOD1) and whether obtained from 8 or 18 week-old animals. Neurospheres formed from epSPCs from the three mouse strains at both 8 (data not shown) and 18 weeks, did not differ in appearance, size or nestin reactivity (Fig. 2A).

To obtain sufficient cells for further analysis and ensure that cultures were devoid of cells not forming neurospheres, we expanded them for 50 days, dissociating them into single-cell suspensions every seven days and re-plated at lower density. After 20 and 50 days we assessed neurosphere cell viability by dissociation into single cells and counting the numbers that did not take up Trypan blue. Similar numbers of viable cells after 20 and 50 days in culture were produced from all the three mouse strains for material taken at week 8 (Fig. 2B). However, for cells taken at postnatal week 18, cell number after 50 days was greater in G93A-SOD1 mice (mean ± SD 14.3 ± 0.4 x 105) than B6.SJL mice (12.4 ± 1.4 x 105, $p<0.05$) and WT-SOD1 (12.1 ± 1.7 x 105, $p<0.05$) (Fig. 2B).

Differentiation of G93A-SOD1 epSPCs produces the three neural lineages in different proportions and morphologies to control epSPCs.
We next assessed the differentiation potential of epSPCs from G93A-SOD1 and controls. In all cases, following growth factor removal, the cells differentiated spontaneously into neurons, astrocytes, and oligodendrocytes, as shown by morphology and immunoreactivity

with anti-NeuN (data not shown), anti-β-tubulin III, anti-GFAP and anti-O4 antibodies, respectively (Fig. 3A). This pluripotency was observed in cells taken from both 8 and 18 wk-old animals, so even at late disease stage, G93A-SOD1 epSPCs had not lost their pluripotency (Fig. 3A). However, the proportions of differentiated cell types differed between disease and control groups (Fig. 3B): in cultures originally isolated at wk 8, neurons formed a slightly greater proportion of G93A-SOD1 epSPCs than control epSPCs (mean % ± SD = 56 ± 5.3 vs. 45.7 ± 7.2 for B6.SJL and 44.3 ± 5.3 for WTSOD1; Fig. 3B). The proportions of astrocytes and oligodendrocytes were correspondingly lower in G93A-SOD1 epSPCs (mean % astrocytes ± SD = 37.5 ± 7 vs. 58.5 ± 20 for B6.SJL and 55.2 ± 13.3 for WT-SOD1, $p<0.01$; mean % oligodendrocytes ± SD = 12 ± 8.1 vs. 19.5 ± 4.2 for B6.SJL and 16.2 ± 2.2 for WT-SOD1; Fig. 3B). For cells originally isolated at wk 18, the proportion of neurons increased further in G93A-SOD1 (mean % ± SD = 69.7 ± 4.9; Fig. 3B) compared to controls (mean ± SD = 40.7 ± 11.9 for B6.SJL and 42.8 ± 4.9 for WT-SOD1, $p<0.001$; Fig .3B and those taken at wk 8 ($p<0.01$), accompanied by a further decrease in astrocyte proportion (mean % ± SD = 20.2 ± 6.6 vs. 56 ± 16.8 for B6.SJL and 60 ± 8.8 for WT-SOD1, $p<0.001$; Fig. 3B). The proportion of oligodendrocytes did not differ with age or mouse strain (Fig. 3B).

We next explored the morphology of neurons and astrocytes: 8-wk-old G93A-SOD1 neurons were morphologically similar to those derived from controls; however, neurons derived from 18-wk-old G93A-SOD1 were smaller than 18-wk-old control neurons as shown by measurement of cell body perimeter (mean ± SD = 12.5 ± 2.4 vs.

30.3 ± 7.3 for WT-SOD1, $p<0.001$; Figs. 3A and 4B $p<0.001$) and than 8-wk-old G93A-SOD1(mean ± SD = 19.9 ± 3.9, $p<0.001$; Figs. 3A and 4B).

We also analyzed the expression of synaptic components in neurons. Most β-tubulin III+ neurons, from 8 and 18 wk-old G93A-SOD1 and control animals, expressed the NMDA-R 2A/B and synaptophysin (Fig. 4A), indicating that cells from diseased and control mice can reach late stages of neuronal differentiation. G93A-SOD1 astrocytes had an activated phenotype as evidenced by thicker processes, at wks 8 and 18, and greater GFAP immunoreactivity than astrocytes derived from age-matched control mice (Fig. 3A, C); GFAP intensity did not change from wk 8 to wk 18 in G93A-SOD1 (or control) astrocytes (Fig. 3C), indicating no further increase in astrocyte activation as the disease progressed.

Expression of differentiation and stem-cell-proliferation miRNAs in G93A-SOD1 epSPCs differs from that in WT-SOD1 and B6.SJL epSPCs

We next investigated the role of miRNAs in epSPC differentiation. We analyzed miR-9, miR-124a, miR-19a and miR-19b expression levels in undifferentiated and differentiated epSPCs from G93ASOD1 and controls (Fig. 5). At wk 8 miR-9 and miR-124a tended to be expressed at higher levels (not significant) in undifferentiated G93A-SOD1 cells than controls; in differentiated cultures miR-9 was higher (not significant) in G93A-SOD1 than B6.SJL and WT-SOD1, and miR-124a was significantly decreased compared to levels in undifferentiated G93A-SOD1 cells ($p<0.0001$) at levels similar to

those in controls. At wk 18, miR-9 was lower in undifferentiated G93A-SOD1 cells than controls($p<0.05$ versus B6.SJL), but significantly higher in differentiated G93A-SOD1 cells than in undifferentiated G93A-SOD1 cells (around 1000 fold, $p<0.0001$), differentiated controls ($p<0.001$) and differentiated 8-wk-old G93A-SOD1 cells ($p<0.001$). miR-124a expression was significantly higher in undifferentiated G93A-SOD1 cultures than B6.SJL ($p<0.01$), while in differentiated cells it was expressed at higher levels in G93A-SOD1 than controls ($p<0.001$) and than differentiated 8- wk-old G93A-SOD1 cells ($p<0.001$).

Levels of miR-19a did not differ between diseased and control cells taken at wk 8, irrespective of differentiation status, but significantly increased from wk 8 to wk 18 in differentiated G93A-SOD1 cultures ($p<0.001$ versus age-matched differentiated controls, and 8-wk-old G93A-SOD1 cultures), and versus undifferentiated G93A-SOD1 cells at wk 18 ($p<0.0001$). miR-19a levels did not differ between 8 and 18 wks in controls.

Levels of miR-19b were similar in undifferentiated 8-wk-old G93A-SOD1 and control cells, but

were significantly higher in differentiated cultures taken at 8 wks than in undifferentiated cultures, both for disease ($p<0.0001$) and control cells ($p<0.001$, WT SOD1; $p<0.05$ B6.SJL). At wk 18 miR-19b levels were significantly lower in undifferentiated G93A-SOD1 cells compared to controls ($p<0.001$), while after differentiation the levels in G93A-SOD1 cells significantly increased compared to the undifferentiated ($p<0.05$) reaching a value similar to those detected in controls.

Changes in miRNA expression in G93A-SOD1 spinal cord as disease develops

Differences in miRNA expression between G93A-SOD1 and controls in cultured epSPCs following differentiation suggested there might that miRNA expression might also differ in spinal cord. We therefore assessed miRNA expression in samples of cervical, thoracic, and lumbar spinal cord taken at wks 8 and 18. We found that miR-9 levels in cervical and thoracic spinal cord, did not differ either between disease and control groups or between time points (Fig. 6). However, levels in G93A-SOD1 lumbar spinal cord taken at wk 18 were decreased compared to wk 8 ($p<0.01$).

Furthermore miR-9 levels in G93A-SOD1 lumbar spinal cord were significantly lower than controls ($p<0.01$ and $p<0.05$) at both ages (Fig. 6).

Levels of miR-124a in the cervical region did not differ between disease and controls or between wk 8 and wk 18. In the thoracic region, miR-124a levels in G93A-SOD1 were significantly decreased at wk 18 compared to wk 8 ($p<0.05$) and at wk 8 compared to age-matched WT-SOD1

($p<0.05$). In the lumbar region miR-124a expression at wk 8 and at wk 18 was significantly lower in G93A-SOD1 than controls ($p<0.05$).

Levels of miR-19a were significantly higher in G93A-SOD1 mice than controls ($p<0.05$) in all spinal cord regions at wk 8 (Fig. 6). At wk 18 miR-19a levels were still higher in G93A than controls in the cervical region ($p<0.05$), but in the thoracic region they were

significantly lower in G93A-SOD1 mice than WT-SOD1 ($p<0.05$; Fig. 6).

Levels of miR-19b did not differ between disease and control groups at wk 8 in any spinal cord region, or at wk 18 in the thoracic region (Fig. 6). In the cervical and lumbar regions, however, miR19b levels at wk 18 were significantly higher in G93A-SOD1 mice than controls ($p<0.01$; Fig. 6), and in the lumbar region, were significantly higher than levels in 8-wk-old G93A-SOD1 mice ($p<0.01$).

Discussion

Motor neuron function might be restored in ALS by promoting neurogenesis from the NSCs present in adult CNS. In contrast to other neurodegenerative disorders, however, there is littleevidence that neurogenesis actually occurs in ALS [36] although studies on G93A-SOD1 miceindicate that the potential for neural regeneration exists in these animals [8,37]. In particular, stem cell proliferation and migration from the ependymal zone of adult spinal cord was found to be much greater in symptomatic than asymptomatic G93A-SOD1 mice, especially in the lumbar region [8,37,38]. The findings of our study support this idea, since significantly greater numbers of neural stem/progenitor cells were present in and around the ependymal zone of lumbar spinal cord of 18-wk-old animals than 8-wk-old animals; numbers of these cells did not change with age in control mice confirming that these cells are normally quiescent [38,39].

We also found that the proliferation ability of G93A-SOD1 epSPCs was enhanced relative to control epSPCs, particularly at late-disease stage. This situation differs from that of rat epSPCs isolated a week

after spinal cord injury, they proliferated in culture at a much higher rate than those from uninjured controls [34]. Thus G93A-SOD1 epSPCs appear to be activated in late stage disease, but not to the extent or in the same way that they are activated by spinal cord injury.

Multilineage differentiation epSPCs in vitro has been demonstrated in mice and rats [34,40] and in the latter is skewed towards glial fate [8,34]. Our in vitro data revealed that over 50% of control differentiated epSPCs expressed GFAP (which is unlikely to be marking stem cells in these cultures as they had been maintained in differentiating medium for 25 days and is reported not to be expressed by adult murine epSPCs [39]). Our control cultures also produced some oligodendrocytes, but over 40% differentiated to neurons.

By contrast, differentiated G93A-SOD1 epSPCs produced more neurons and fewer astrocytes than controls, and the proportion of neurons further increased (and astrocytes decreased) in late stage disease, suggesting that neural fate programming might be altered in these mice.

The G93A-SOD1 astrocytic cells were more activated (thicker processes and greater GFAP immunoreactivity) [40] than differentiated control cells, at both asymptomatic and symptomatic time points. Another study found greater numbers of activated astrocytes in G93A-SOD1 mice than non-transgenic controls throughout the animals' lifespan [41]. A more recent study found that primary cortical astrocytes cultured from neonatal G93A-SOD1 mice were highly prone to enter an activated neuroinflammatory state [42]. While activated astrocytes seem to be involved in endogenous repair following brain injury, [40] those carrying an ALS-causing mutation

have a pathologic role in ALS, in that they show specific toxicity towards motor neurons [10,43].

As regards neurons differentiated from G93A-SOD1 epSPCs, those isolated at wk 18 were significantly smaller than those from control epSPCs. Interestingly, in dissociated spinal cord cultures, most small-size neurons positive for Hb9 (motor neuron marker) were negative for markers of mature neurons (non-phosphorylated neurofilament and choline acetyltransferase) [44].

By confocal microscopy of G93A-SOD1 mouse lumbar spinal cord at late-stage disease, residual motor neurons tended to be smaller than typical α-motor neurons [45]. Taken together, these data suggest that epSPC-derived neurons in G93A-SOD1 mouse are less mature than their control counterparts.

Our hypothesis that neural fate programming is altered in G93A-SOD1 mice is reinforced by changes in miR-9 and miR-124a expression on epSPC differentiation in vitro. Both miRNAs were highly upregulated in differentiated G93A-SOD1 epSPCs isolated at wk 18 compared to wk 8, whereas changes in expression following differentiation of control epSPCs were small or nonexistent.

Krichevsky et al. [13] showed that upregulation of miR-9 and miR-124 leads to reduced in vitro differentiation of stem cells along the astrocytic lineage, with commensurate increase in differentiation along the neuronal lineage. While miR-9 exerts different effects on proliferation, migration and differentiation of neural progenitor cells in a context-dependent manner [46,47], miR-124 is clearly involved in neuronal differentiation and is also expressed in mature neurons [14].

miR-9 expression was also highly altered in the lumbar region of G93A-SOD1 mouse spinal cord in comparison with controls. In contrast to our findings on differentiation in vitro (where miR-9 was highly upregulated) this miRNA was significantly downregulated in diseased lumbar spinal cord at wk 18, supporting histological observations indicating that reactive astrogliosis is increased in the G93A-SOD1 lumbar spinal cord [8,41]. Similarly, the downregulated miR-124a expression in 18-wk-old G93A-SOD1 spinal cord is consistent with the few sporadic Dlx2-positive cells we observed in wk 18 spinal cord, and also consistent with the findings of Guan et al. [8] in the same animal model, that no new neurons were produced. Our study has shown, however, that while G93A-SOD1 epSPCs can differentiate into neurons in vitro, and at least some of the appropriate miRNA differentiation signals are present in vivo, these signals are repressed in vivo, as conjectured by Guan et al [8].

Our findings on altered miR-19a and -19b expression in G93A-SOD1 mice is potentially relevant to human ALS since G1 to S phase cell-cycle regulators are altered in ALS possibly because cell cycle proteins are altered and these are predicted targets of miR-19a and miR-19b regulation [48].

We propose that the greatly increased numbers of epSPCs in spinal cord do not give rise to new neurons in vivo, either because differentiation is blocked by altered neural cell fate programming, or because differentiating epSPCs die, due to an improper cell cycle activation [48].

The network representation of Gene Ontology, KEGG, and BioCarta functional annotation terms of genes that are targeted by the miRNAs

studied is presented in Figure 7; it recapitulates the possible involvement of the studied miRNAs in functions associated with neurogenesis, to which participate the gene targets they were shown to regulate experimentally. It should be kept in mind that, while the role of miRNAs is generally thought to be one of gene repression, enhancement of translation by miRNAs has also been demonstrated [49,50,51], and the mode of action by which the miRNA we have studied could affect neurogenesis in G93A-SOD1 mice, in particular by altering neural cell fate, is as yet unclear. Nevertheless, it can be seen that each of the studied miRNAs can affect more than one function relevant to neurogenesis, either by targeting more than one gene relevant to a particular function or through a unique target that has repercussions on several pathways. One of the most studied CNS-associated miRNA, miR-124a, targets a number of genes (Fig. 7). A recent study validated miR-124a as a regulator of adult neurogenesis in brain subventricular zone (SVZ) stem cell niche, through direct targeting of Jag1, Dlx2 and SOX9; in particular, downregulation of SOX9 was shown to be required for neurogenesis and its overexpression maintained SVZ cells as GFAP-positive astrocytes and completely eliminated neuronal production [14]. Both miR-124a and miR-9 could be involved directly or indirectly in the regulation of the cell-function signaling pathways responsible for cell survival and neurogenesis, through regulation of Stat3 signaling (Fig. 7). MiR-9 was shown to promote the differentiation of mesenchymal stem cells into neurons through Notch signaling [18]; it is involved in neural stem cell fate determination through a feedback regulatory loop with the nuclear receptor TLX [30] and can coordinate proliferation and

migration choices in human neural progenitor cells through targeting stathmin [16]. Both TLX (Nr2e1) and stathmin (Stmn1), as well as Hes1 which plays a crucial role in maintaining neural progenitors [46], are linked directly or indirectly through Jag1 to the Notch signaling pathway (Fig. 7). It can be seen from Figure 7 that miR-19a and -19b through their targeting Pten [31], Ccnd2 [52], and/or SOCS-1 [53], are highly involved in regulation of pathways associated with modulation of the cell cycle and with cell arrest and apoptosis. We therefore suggest that they might be involved in cell arrest and/or death of progenitors arising from epSPCs, a process that might result from the highly inflammatory environment at this stage of the disease [54].

Factors negatively influencing miRNA expression in G93A-SOD1 spinal cord, particularly when the disease is severe, remain to be investigated. It is known that an inflammatory environment prevails in the spinal cord of these mice [41,42] and could well influence miRNA expression, as occurs for example in the multiple sclerosis mouse model: during active CNS inflammation both microglia and macrophages expressing markers of the classical pathway (mediated by Th1 cytokines) had low levels of miR-124 [55]. The effects of the mutated SOD1 must also be considered. We speculate that high levels of hydroxyl radical, produced by mutant enzyme [56] might interfere with the nitric oxide signalling involved in the differentiation of neuronal precursors to mature neurons [57], and could in turn influence miRNA expression. However, further studies are required to firm-up the hypothesis.

Overall our findings link lack of neurogenesis in the spinal cord of 18-wk-old G93A-SOD1 mice to defective expression of miRNAs involved in neuronal differentiation and cell cycle regulation. We propose epSPCs (and neurospheres) isolated from G93A-SOD1 as an in vitro model for investigating ALS pathogenesis and new therapeutic agents since these cells seem to retain a memory (altered neural fate programming) of the dysregulated spinal cord.

Acknowledgement: We are very grateful to Drs. F. Navone and N. Borgese (Consiglio Nazionale delle Ricerche Institute of Neuroscience, Milan, Italy) and to Dr. V. Moreno-Manzano (Neural Regeneration Lab, Centro de Investigacion "Principe Felipe", Valencia, Spain) for helpful discussions and critical reading of the manuscript; Dr. D. Locatelli and Dr. G. Battaglia (Division of Neuropathology, Istituto Neurologico "Carlo Besta", Milan, Italy) for the kind gift of antisynaptophysin and anti-NMDA receptor 2A/B antibodies. The authors thank Don Ward for critical discussion and help with the English. This work was supported by the Italian Ministry of Health Grant No. RF-INN-2007-644440 to R.M.; Italian Ministry of Health Annual Research Funding (RC2010/LR3 and RC2011/LR3) to R.M.; 8598/Ricerca Indipendente 2009/Regione Lombardia to R.M.

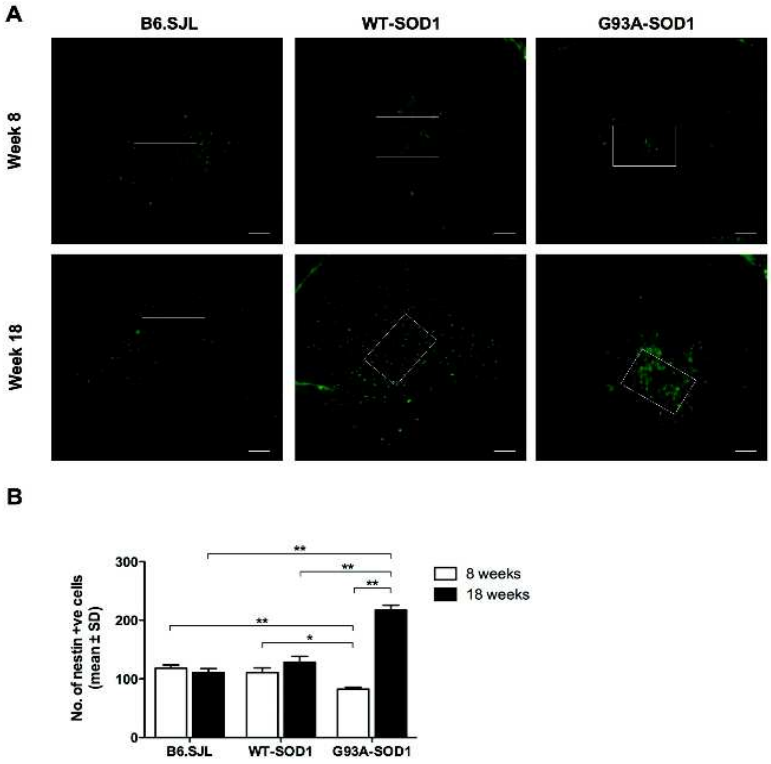

Fig. 1. Nestin-positive cells are more numerous in ependymal zone of G93A-SOD1 mouse spinal cord at postnatal 18 week than week 8. (A) Photomicrographs showing nestin immunostaining of lumbar spinal cord at postnatal weeks 8 and 18 in B6.SJL, WT-SOD1 and G93A-SOD1 mice. The rectangle illustrates the size of area in which nestin-positive cells in and around the ependymal zone were counted (magnification x10). (B) Quantification of nestin-positive cells in and around the ependymal zone of B6.SJL, WT-SOD1 and G93A mouse spinal cord, expressed as mean number ± SD of nestin-positive cells in rectangle from 20 lumbar spinal cord sections per mouse with three mice analyzed per mouse strain. *$p<0.05$ and **$p<0.001$, ANOVA and Bonferroni post-hoc. Scale bar = 25μm

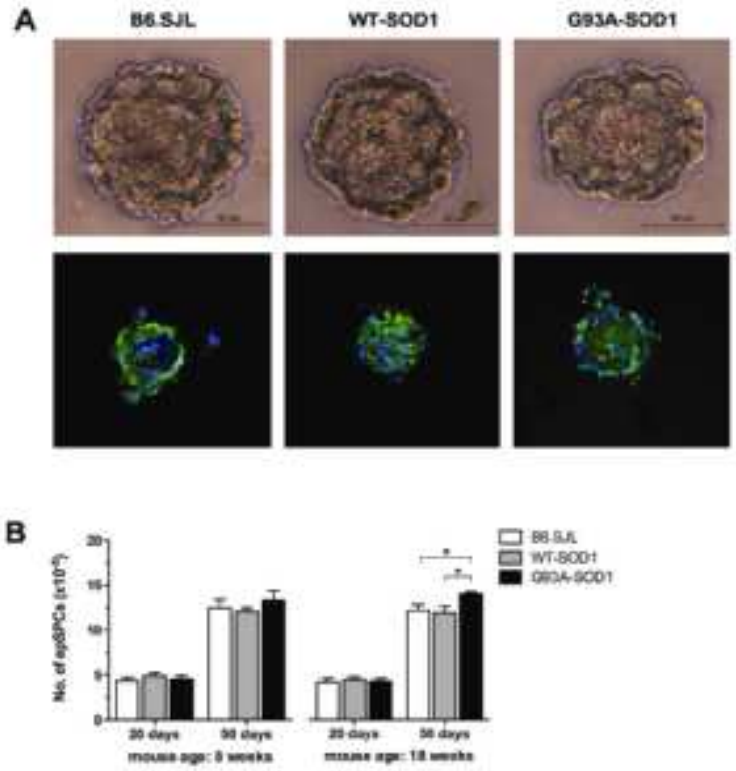

Fig. 2. The proliferation potential of G93A-SOD1 epSPCs at late disease stage is slightly greater than in controls. (A) Photomicrographs of neurospheres cultured from 18-week-old B6.SJL, WTSOD1 and G93A-SOD1 spinal cord for 50 days. Upper panel, optical microscopy; lower panel, confocal microscopy with double-staining for nestin (green) and DAPI (blue). (B) Quantification of viable cells dissociated from neurospheres after 20 and 50 days in culture originally isolated from mouse spinal cord at weeks 8 and 18. Data are means ± SD of 6 mice per strain, 1 culture from each mouse. *p<0.05, ANOVA and Bonferroni post-hoc. Scale bar = 50μm

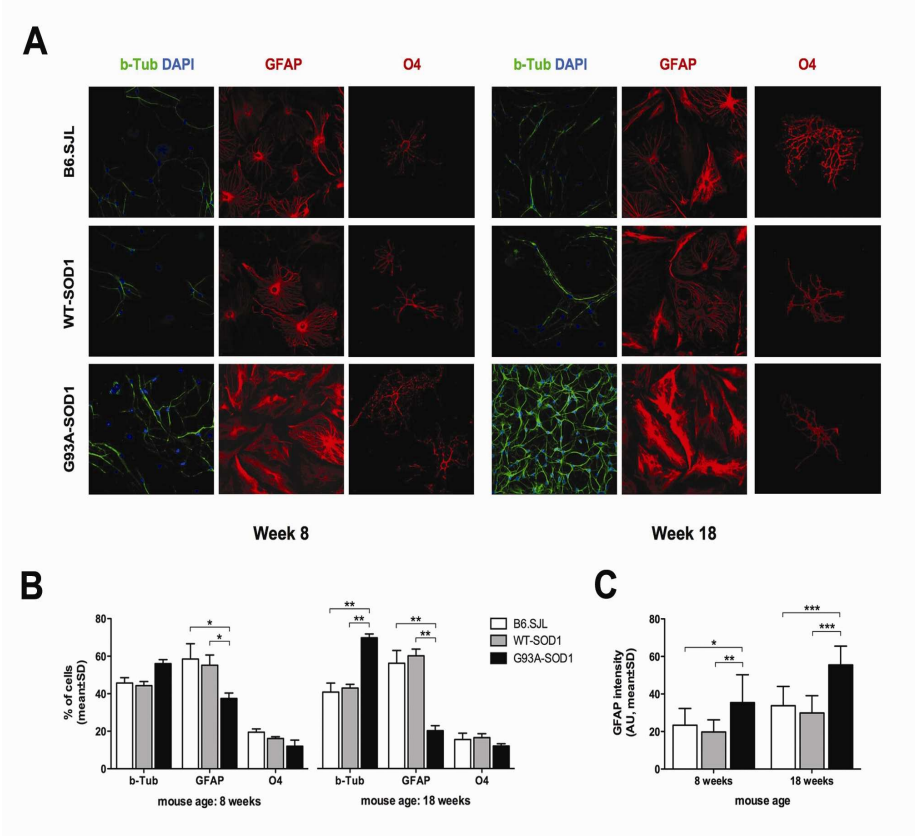

Fig. 3. Differentiation of epSPCs into three neural lineages showed a higher percentage of neurons and more activated astrocytes in cells derived from G93A-SOD1 than in those derived from agematched controls. (A) Confocal microscopy images of B6.SJL, WT-SOD1 and G93A-SOD1 epSPCs cells isolated at week 8 or 18, cultured as neurospheres for 50 days, dissociated, differentiated for 25 days, and stained for neuronal (β-tubulin III, counterstained DAPI), astrocytic (GFAP), and oligodendrocytic (O4) cells. (B) Quantification of differentiated cells from B6.SJL, WT-SOD1 and G93A-SOD1 epSPCs at week 8 and 18 of age. Data are mean % ± SD (separate cultures, 6 mice per strain) of DAPI-stained cells positive for

either β-tubulin III (b-Tub), GFAP, and O4. *p<0.01, **p<0.001 ANOVA and Bonferroni post-hoc. (C) Quantification of GFAP immunoreactivity in astrocytes from 8- and 18 week-old B6.JSL, WT-SOD1 and G93A mice. Data, expressed as percentage of intensity relative to the delimited area, are mean (± SD) of staining intensity obtained throughout the length of single astrocytes present in 10 randomly selected fields per coverslip (8 coverslips per culture, 6 cultures for each animal group). *p<0.05; **p<0.01,*** p<0.001 ANOVA and Bonferroni post-hoc. Scale bar = 10 μm.

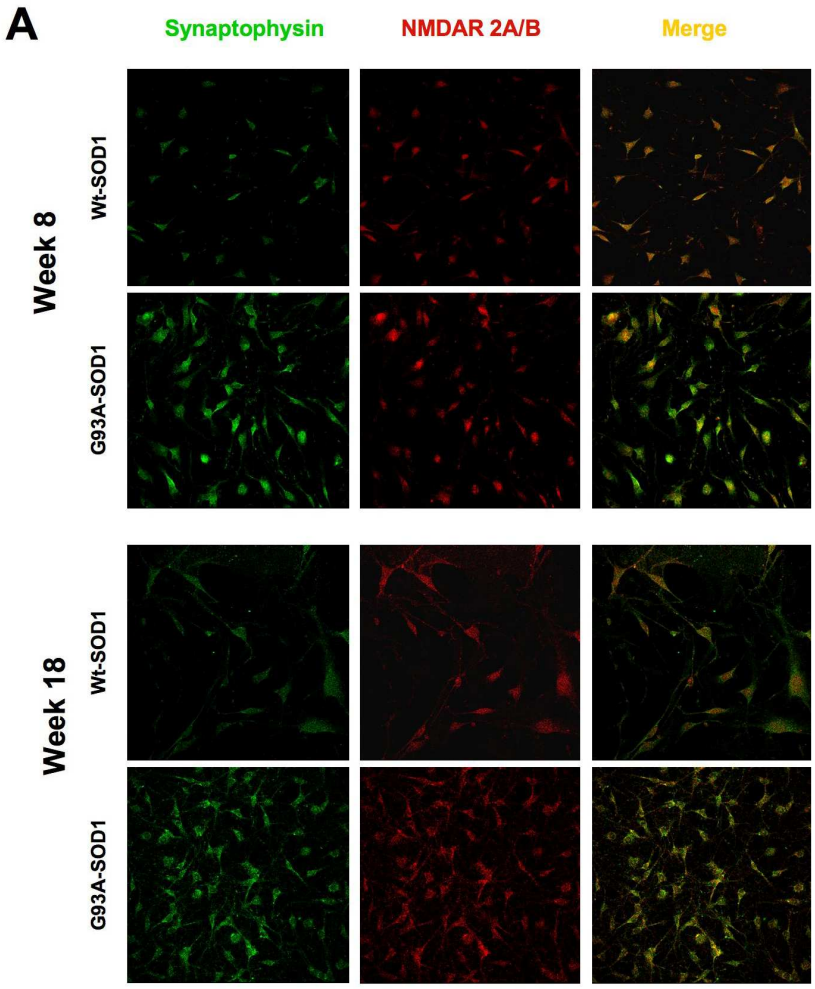
A
Synaptophysin
NMDAR 2A/B
Merge
Week 8
Wt-SOD1
G93A-SOD1
Week 18
Wt-SOD1
G93A-SOD1

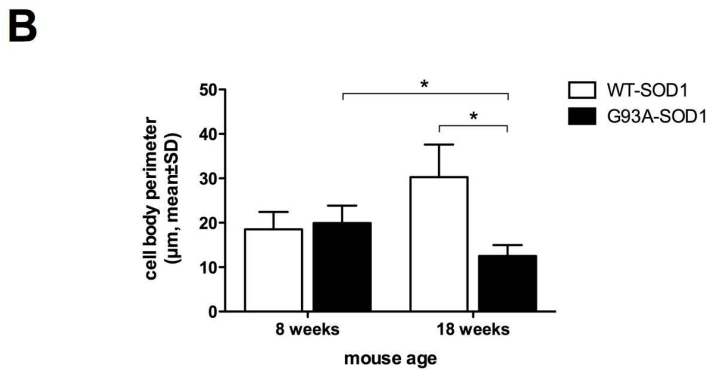
B
cell body perimeter (µm, mean±SD)
50
40
30
20
10
0
*
*
WT-SOD1
G93A-SOD1
8 weeks
18 weeks
mouse age

Fig. 4. 18-week-old G93A-SOD1 epSPC-derived neurons were smaller than those derived from age-matched WT-SOD1 mice. (A) Confocal microscopy images of WT-SOD1 and G93A-SOD1 epSPCs isolated at week 8 or 18, cultured as neurospheres for 50 days, dissociated, differentiated for 25 days, and stained for two markers of mature neurons: synaptophysin (green) and NMDA receptor 2A/B (red). (B) Quantification of neuronal body perimeter. Data, expressed in μm, are mean (±SD) of cell perimeter (separate cultures from 3 mice per strain, 3 slides per culture, 5 randomly chosen fields per slide). *P<0.001 ANOVA and Bonferroni post-hoc. Scale bar: 15 μm.

FIG. 5. Altered expression of miRNAs involved in neural cell fate (miR-9 and miR-124a) and cellcycle regulation (miR-19a and miR-19b) in G93A-SOD1 epSPCs. Real-time RT-PCR measurements of miRNA expression levels in undifferentiated and differentiated epSPCs isolated from spinal cord of B6.SJl (white bars), WT-SOD1 (light gray bars), G93A-SOD1 (black bars) at weeks 8 (n = 5 animals per group) and 18 (n = 5 animals per group). Relative expression data are presented as mean ± SD, *p<0.05; **p<0.01; ***p<0.001.

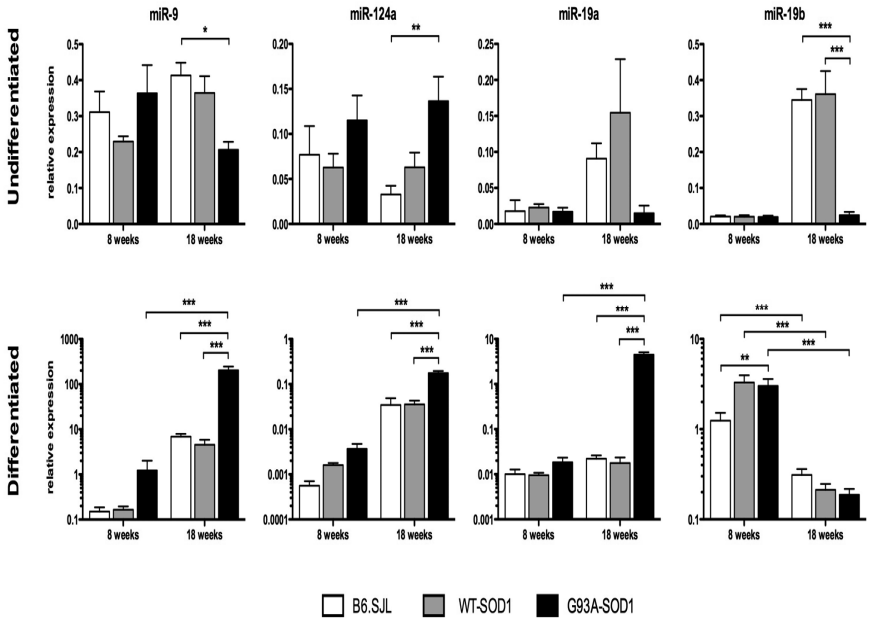

Fig. 5. Altered expression of miRNAs involved in neural cell fate (miR-9 and miR-124a) and cell-cycle regulation (miR-19a and miR-19b) in G93A-SOD1 epSPCs. Real-time RT-PCR measurements of miRNA expression levels in undifferentiated and differentiated epSPCs isolated from spinal cord of B6.SJl (white bars), WT-SOD1 (light gray bars), G93A-SOD1 (black bars) at weeks 8 (n = 5 animals per group) and 18 (n = 5 animals per group). Relative expression data are presented as mean ± SD, *p<0.05; **p<0.01; ***p<0.001.

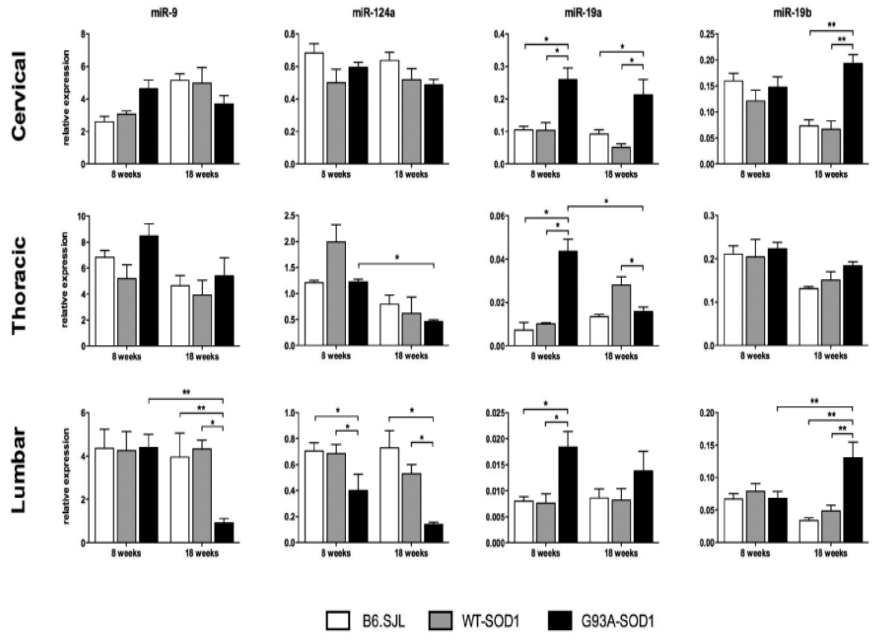

Fig. 6. Altered expression of miRNAs involved in neural cell fate (miR-9 and miR-124a) and cell cycle regulation (miR-19a and miR-19b) in G93A-SOD1 spinal cord. Real-time RT-PCR measurements of miRNA expression levels in cervical, thoracic, and lumbar spinal cord of B6.SJl (white bars), WT-SOD1 (light gray bars), G93A-SOD1 (black bars) at weeks 8 (n = 5 animals per group) and 18 (n = 5 animals per group). Relative expression data are presented as mean ± SD, *p<0.05; **p<0.01; ***p<0.001.

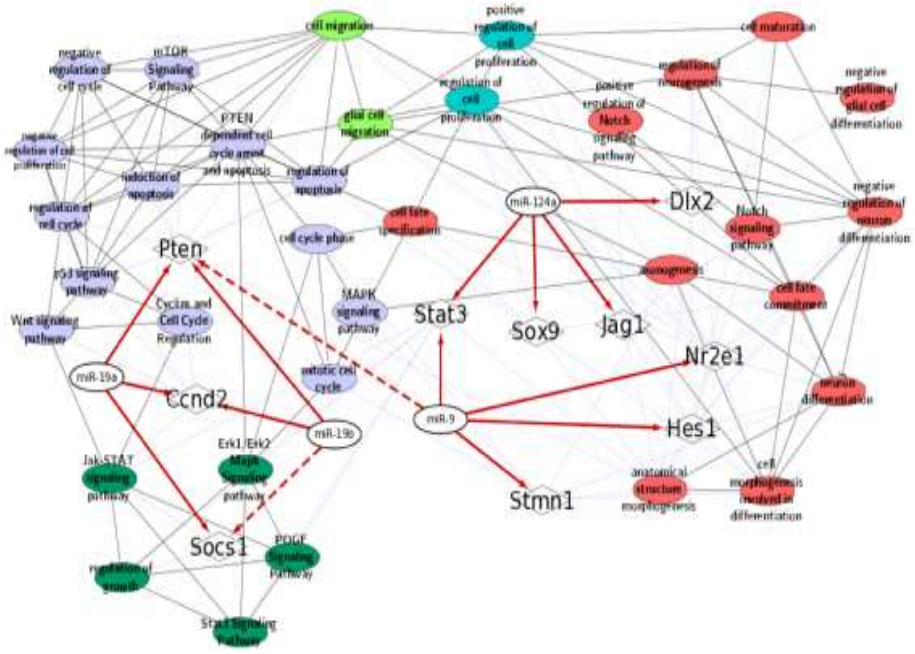

Fig. 7. Network representation of the possible involvement of studied miRNAs in functions relevant to adult neurogenesis, analyzed on the basis of their experimentally validated targets. The targets for the studied miRNAS were selected on the basis of their published experimental validation. The network was constructed using the Cytoscape software through the ClueGO plug-in and was further customized manually to show inhibition of the validated targets by the relevant miRNAs studied. Pten and SOCS-1 were also predicted as targets of miR-9 and miR-19b, respectively using the DIANA-microT-3.0-Strict algorithm through the DIANA miRNA database (http://diana.cslab.ece.ntua.gr/microT/).

REFERENCES

1. Andersen PM and A Al-Chalabi. (2011). Clinical genetics of amyotrophic lateral sclerosis: what do we really know? Nat Rev Neurol 7:603–615.

2. Gruzman A, WL Wood, E Alpert, MD Prasad, RG Miller, JD Rothstein, R Bowser, R Hamilton, TD Wood, Don W Cleveland, VR Lingappa and J Liu. (2007). Common molecular signature in SOD1 for both sporadic and familial amyotrophic lateral sclerosis. Proc Natl Acad Sci 104:12524–12529.

3. Gurney ME. (1997). The use of transgenic mouse models of amyotrophic lateral sclerosis in preclinical drug studies. J Neurol Sci 152 Suppl 1:S67–73.

4. Marcuzzo S, I Zucca, A Mastropietro, N Kerlero de Rosbo, P Cavalcante, S Tartari, S Bonanno, L Preite, R Mantegazza and P Bernasconi. (2011). Hind limb muscle atrophy precedes cerebral neuronal degeneration in G93A-SOD1 mouse model of amyotrophic lateral sclerosis: a longitudinal MRI study. Exp Neurol 231:30–37.

5. Boulis NM, T Federici, JD Glass, JS Lunn, SA Sakowski and EL Feldman. (2011). Translational stem cell therapy for amyotrophic lateral sclerosis. Nat Rev Neurol 8:172–176.

6. Lie DC, H Song, SA Colamarino, GL Ming and FH Gage. (2004). Neurogenesis in the adult brain: new strategies for central nervous system diseases. Annu Rev Pharmacol Toxicol 44:399–421.

7. Curtis MA, M Kam and RL Faull. (2011). Neurogenesis in humans. Eur J Neurosci 33:1170–1174.

8. Guan YJ, X Wang, HY Wang, K Kawagishi, H Ryu, CF Huo, EM Shimony, BS Kristal, HG Kuhn and RM Friedlander. (2007). Increased stem cell proliferation in the spinal cord of adult amyotrophic lateral sclerosis transgenic mice. J Neurochem 102:1125–1138.

9. Foret A, R Quertainmont, O Botman, D Bouhy, P Amabili, G Brook, J Schoenen and R Franzen. (2010). Stem cells in the adult rat spinal cord: plasticity after injury and treadmill training exercise. J Neurochem 112:762–772.

10. Haidet-Phillips AM, ME Hester, CJ Miranda, K Meyer, L Braun, A Frakes, S Song, S Likhite, MJ Murtha, KD Foust, M Rao, A Eagle, A Kammesheidt, A Christensen, JR Mendell, AH Burghes and BK Kaspar. (2011). Astrocytes from familial and sporadic ALS patients are toxic to motor neurons. Nat Biotechnol 29:824–828.

11. Makeyev EV and T Maniatis. (2008). Multilevel regulation of gene expression by microRNAs. Science 319:1789–1790.

12. Liu C and X Zhao. (2009). MicroRNAs in adult and embryonic neurogenesis. Neuromolecular Med 11:141–152.

13. Krichevsky AM, KC Sonntag, O Isacson and KS Kosik. (2006). Specific microRNAs modulate embryonic stem cell-derived neurogenesis. Stem Cells 24:857–864.

14. Cheng LC, E Pastrana, M Tavazoie and F Doetsch. (2009). miR-124 regulates adult neurogenesis in the subventricular zone stem cell niche. Nat Neurosci 12:399–408.

15. Shen Q and S Temple. (2009). Fine control: microRNA regulation of adult neurogenesis. Nat Neurosci 12:369–370.

16. Delaloy C, L Liu, JA Lee, H Su, F Shen, GY Yang, WL Young, KN Ivey and FB Gao. (2010). MicroRNA-9 coordinates proliferation and migration of human embryonic stem cell-derived neural progenitors. Cell Stem Cell 6:323–335.

17. Li X and P Jin. (2010). Roles of small regulatory RNAs in determining neuronal identity. Nat Rev Neurosci 11:329–338.

18. Jing L, Y Jia, J Lu, R Han, J Li, S Wang and T Peng. (2011). MicroRNA-9 promotes differentiation of mouse bone mesenchymal stem cells into neurons by Notch signaling. Neuroreport 22:206–211.

19. De Smaele E, E Ferretti and A Gulino. (2010). MicroRNAs as biomarkers for CNS cancer and other disorders. Brain Res 1338:100–111.

20. Haramati S, E Chapnik, Y Sztainberg, R Eilam, R Zwang, N Gershoni, E McGlinn, PW Heiser, AM Wills, I Wirguin, LL Rubin, H Misawa, CJ Tabin, R Brown, A Chen and E Hornstein. (2010). miRNA malfunction causes spinal motor neuron disease. Proc Natl Acad Sci U S A 107:13111–13116.

21. Satoh J. (2010). MicroRNAs and their therapeutic potential for human diseases: aberrant microRNA expression in Alzheimer's disease brains. J Pharmacol Sci 114:269–275.

22. Williams AH, G Valdez, V Moresi, X Qi, J McAnally, JL Elliott, R Bassel-Duby, JR Sanes and EN Olson. (2009). MicroRNA-206 delays ALS progression and promotes regeneration of neuromuscular synapses in mice. Science 326:1549–1554.

23. Jiang YM, M Yamamoto, Y Kobayashi, T Yoshihara, Y Liang, S Terao, H Takeuchi, S Ishigaki, M Katsuno, H Adachi, J Niwa, F Tanaka, M Doyu, M Yoshida, Y Hashizume and G Sobue. (2005).

Gene expression profile of spinal motor neurons in sporadic amyotrophic lateral sclerosis. Ann Neurol 57:236–251.

24. Kirby J, E Halligan, MJ Baptista, S Allen, PR Heath, H Holden, SC Barber, CA Loynes, CA Wood-Allum, J Lunec and PJ Shaw. (2005). Mutant SOD1 alters the motor neuronal transcriptome: implications for familial ALS. Brain 128:1686–1706.

25. Ferraiuolo L, PR Heath, H Holden, P Kasher, J Kirby and PJ Shaw. (2007). Microarray analysis of the cellular pathways involved in the adaptation to and progression of motor neuron injury in the SOD1 G93A mouse model of familial ALS. J Neurosci 27:9201–9219.

26. Makeyev EV, J Zhang, MA Carrasco and T Maniatis. (2007). The MicroRNA miR-124 promotes neuronal differentiation by triggering brain-specific alternative pre-mRNA splicing. Mol Cell 27:435–448.

27. Visvanathan J, S Lee, B Lee, JW Lee and SK Lee. (2007). The microRNA miR-124 antagonizes the anti-neural REST/SCP1 pathway during embryonic CNS development. Genes Dev 21:744–749.

28. Ponomarev ED, T Veremeyko, N Barteneva, AM Krichevsky and HL Weiner. (2011). MicroRNA-124 promotes microglia quiescence and suppresses EAE by deactivating macrophages via the C/EBP-α-PU.1 pathway. Nat Med 17:64–70.

29. Gao FB. (2010). Context-dependent functions of specific microRNAs in neuronal development. Neural Dev 5:25–33.

30. Zhao C, G Sun, S Li and Y Shi. (2009). A feedback regulatory loop involving microRNA-9 and nuclear receptor TLX in neural stem cell fate determination. Nat Struct Mol Biol 16:365–371.

31. Olive V, MJ Bennett, JC Walker, C Ma, I Jiang, C Cordon-Cardo, QJ Li, SW Lowe, GJ Hannon and L He. (2009). miR-19 is a key oncogenic component of mir-17-92. Genes Dev 23:2839–2849.

32. Stadler B, I Ivanovska, K Mehta, S Song, A Nelson, Y Tan, J Mathieu, C Darby, CA Blau, C Ware, G Peters, DG Miller, L Shen, MA Cleary and H Ruohola-Baker. (2010). Characterizatio of microRNAs involved in embryonic stem cell states. Stem Cells Dev 19:935–950.

33. Reynolds BA and RL Rietze. (2005). Neural stem cells and neurospheres-re-evaluating the relationship. Nat Methods 2:333–336.

34. Moreno-Manzano V, FJ Rodriguez-Jimenez, M Garcia-Rosello, S Lainez, S Erceg, MT Calvo, M Ronaghi, M Lloret, R Planells-Cases, JM Sanchez-Puelles and M Stojkovic. (2009). Activated spinal cord ependymal stem cells rescue neurological function. Stem Cells 27:733–743.

35. Bindea G, B Mlecnik, H Hackl, P Charoentong, M Tosolini, A Kirilovsky, WH Fridman, F Pages, Z Trajanoski and J Galon. (2009). ClueGO: a Cytoscape plug-in to decipher functionally grouped gene ontology and pathway annotation networks. Bioinformatics 25:1091–1093.

36. Abdipranoto A, S Wu, S Stayte and B Vissel. (2008). The role of neurogenesis in neurodegenerative diseases and its implications for therapeutic development. CNS Neurol Disord Drug Targets 7:187–210.

37. Chi L, Y Ke, C Luo, B Li, D Gozal, B Kalyanaraman and R Liu. (2006). Motor neuron degeneration promotes neural progenitor cell

proliferation, migration, and neurogenesis in the spinal cords of amyotrophic lateral sclerosis mice. Stem Cells 24:34–43.

38. Gage FH. (2000). Mammalian neural stem cells. Science 287:1433–1438.

39. Meletis K, F Barnabe-Heider, M Carlen, E Evergren, N Tomilin, O Shupliakov and J Frisen. (2008). Spinal cord injury reveals multilineage differentiation of ependymal cells. PLoS Biol 6:e182.

40. Escartin C, and G Bonvento. (2008). Targeted activation of astrocytes: a potential neuroprotective strategy. Mol Neurobiol 38:231–241.

41. Hall ED, JA and Oostveen ME Gurney. (1998). Relationship of microglial and astrocytic activation to disease onset and progression in a transgenic model of familial ALS. Glia 23:249–256.

42. Hensley K, H Abdel-Moaty, JHunter, M Mhatre, S Mou, K Nguyen, T Potapova, QN Pye, M Qi, H Rice, C Stewart, K Stroukoff and M West. (2006). Primary glia expressing the G93ASOD1 mutation present a neuroinflammatory phenotype and provide a cellular system for studies of glial inflammation. J Neuroinflammation 3:2.

43. Nagai M, DB Re, T Nagata, A Chalazonitis, TM Jessell, H Wichterle and S Przedborski. (2007). Astrocytes expressing ALS-linked mutated SOD1 release factors selectively toxic to motor neurons. Nat Neurosci 10:615–622.

44. Chang Q and LJ Martin. (2011). Glycine receptor channels in spinal motoneurons are abnormal in a transgenic mouse model of amyotrophic lateral sclerosis. J Neurosci 31:2815–2827.

45. Chang Q and LJ Martin. (2009). Glycinergic innervation of motoneurons is deficient in amyotrophic lateral sclerosis mice: a quantitative confocal analysis. Am J Pathol 174:574-585.
46. Bonev B, A Pisco and N Papalopulu. (2011). MicroRNA-9 reveals regional diversity of neural progenitors along the anterior-posterior axis. Dev Cell 20:19–32.
47. Yuva-Aydemir Y, A Simkin , E Gascon and FB Gao . (2011). MicroRNA-9: functionalevolution of a conserved small regulatory. RNA 8:557–64.
48. Ranganathan S and R Bowser. (2003). Alterations in G(1) to S phase cell-cycle regulators during amyotrophic lateral sclerosis. Am J Pathol 162:823–835.
49. Vasudevan S, Y Tong and JA Steitz. (2007). Switching from repression to activation: microRNAs can up-regulate translation. Science 318:1931–1934.
50. Selbach M, B Schwanhausser, N Thierfelder, Z Fang, R Khanin and N Rajewsky. (2008). Widespread changes in protein synthesis induced by microRNAs. Nature 455:58–63.
51. Tsai NP, YL Lin and LN Wei. (2009). MicroRNA mir-346 targets the 5'-untranslated region of receptor-interacting protein 140 (RIP140) mRNA and up-regulates its protein expression. Biochem J 424:411-418.
52. Lam QL, S Wang, OK Ko, PW Kincade and L Lu. (2010). Leptin signaling maintains B-cell homeostasis via induction of Bcl-2 and Cyclin D1. Proc Natl Acad Sci U S A 107:13812–13817.
53. Pichiorri F, SS Suh, M Ladetto, M Kuehl, T Palumbo, D Drandi, C Taccioli, N Zanesi, H Alder, JP Hagan, R Munker, S Volinia, M

Boccadoro, R Garzon, A Palumbo, RI Aqeilan and CM Croce. (2008). MicroRNAs regulate critical genes associated with multiple myeloma pathogenesis. Proc Natl Acad Sci U S A 105:12885–12890.

54. Diaz-Amarilla P, S Olivera-Bravo, E Trias, A Cragnolini, L Martinez-Palma, P Cassina, J Beckman and L Barbeito. (2011). Phenotypically aberrant astrocytes that promote motoneuron damage in a model of inherited amyotrophic lateral sclerosis. Proc Natl Acad Sci U S A 108:18126–18131.

55. Ponomarev ED, T Veremeyko and HL Weiner. (2012). MicroRNAs are universal regulators of differentiation, activation, and polarization of microglia and macrophages in normal and diseased CNS. Glia doi:10.1002/glia.22363.

56. Andrus PK, TJ Fleck, ME Gurney and ED Hall. (1998). Protein oxidative damage in a transgenic mouse model of familial amyotrophic lateral sclerosis. J Neurochem 71:2041–2048.

57. Mujoo K, JS Krumenacker and F Murad. (2011). Nitric oxide-cyclic GMP signaling in stem cell differentiation. Free Radic Biol Med 51:2150–2157.

Supplementary Information

1. *Supplementary materials*

2. *Supplementary Figure 1*. Detection of neuroblasts in the lumbar spinal cord of G93A-SOD1 and WTSOD1 mice at week 18.

Supplementary. List of reagents and manufacturers Source Working dilution

Reagents for cell culture:

- Collagenase I Life Technologies (Foster City, CA) cell culture
- Matrigel BD Biosciences (San Jose, CA)
- Fetal Bovine Serum Life Technologies (Foster City, CA)

Primary antibodies:

- Mouse anti-mouse nestin IgG antibody Millipore (Billerica, MA) 1:200
- Mouse anti-mouse β-tubulin III IgG antibody Millipore (Billerica, MA) 1:100
- Mouse anti-mouse NeuN antibody IgG Millipore (Billerica, MA) 1:100
- Rabbit anti-mouse glial fibrillary acid protein (GFAP) IgG antibody Dako Cytomation (Glostrup, Denmark) 1:300
- Mouse anti-mouse O4 IgM antibody Millipore (Billerica, MA) 1:100
- Rabbit anti-mouse N-methyl-D-aspartate receptor 2A/B antibody (NMDA) Millipore (Billerica, MA) 1:100
- Mouse anti-mouse synaptophysin IgG antibody Millipore (Billerica, MA) 1:100

- Goat anti-mouse distal-less homeobox 2 (Dlx2) IgG antibody Santa Cruz (Heidelberg, Germany) 1:50

Secondary antibodies:

- Cy3-conjugated goat anti-rabbit IgG Jackson ImmunoResearch (Newmarket, UK) 1:600 antibodies
- Cy3-conjugated goat anti-mouse IgM Jackson ImmunoResearch (Newmarket, UK) 1:600
- Cy2-conjugated goat anti-mouse IgG Jackson ImmunoResearch (Newmarket, UK) 1:200
- Cy2-conjugated donkey anti-goat IgG Jackson ImmunoResearch (Newmarket, UK) 1:200
- DAPI Life Technologies (Foster City, CA) 1:1000
- Isotype-specific non-immune IgG (control) Dako Cytomation (Glostrup, Denmark) 1:200
- Normal goat serum (control) Vector Laboratories (Peterborough, UK)

Reagents for Sample conservation:

- Optical Cutting Temperature Compound Bio-Optica (Milan, Italy)
- FluorSave Reagent Calbiochem (Darmstadt, Germany)

Reagents for qReal-Time PCR:

- Trizol Life Technologies (Foster City, MA)
- TaqMan MicroRNA reverse Transcription Kit Life Technologies (Foster City, MA)
- Mmu-miR-9 Assay ID000583 Life Technologies (Foster City, MA)
- Mmu-miR-124a Assay ID001182 Life Technologies (Foster City, MA)

- Mmu-miR-19a Assay ID000395 Life Technologies (Foster City, MA)
- Mmu-miR-19b Assay ID000396 Life Technologies (Foster City, MA)

2. *Supplementary Figure*

Supplementary Figure

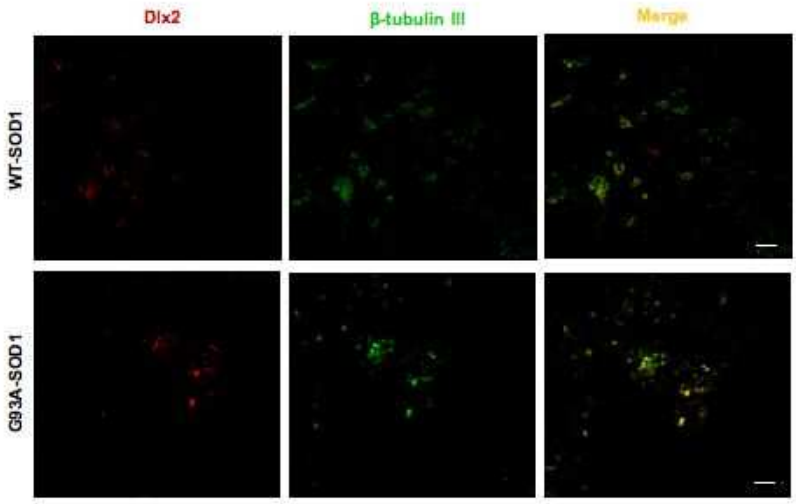

Supplementary Figure 1. **Detection of neuroblasts in the lumbar spinal cord of G93A-SOD1 and WT-SOD1 mice at week 18.** Tissue sections stained with antibodies to Dlx2 (red), marker of neuroblast, and β-tubulin III (green), marker of neurons, showed the presence of a small number of neuroblasts coexpressing Dlx2 and anti-β-tubulin III in G93A-SOD1 mice and in controls without any significant difference between the two groups of animals (scare bar 10μm).

CHAPTER 4

SUMMARY, CONCLUSIONS AND FUTURE PERSPECTIVES

ALS is a progressive neurodegenerative disease affecting motor neurons. Although most cases of ALS are sporadic, a familiar form (10% of patients), mainly caused by mutations of super oxide dismutase1 (SOD1) gene, also exists (Andersen, Al-Chalabi, 2011). In both sporadic and familial ALS forms the same neurons with similar pathology are affected (Gruzman et al., 2007). Selective vulnerability of motor neurons likely arises from a combination of several mechanisms, including protein misfolding, mitochondrial dysfunction, oxidative damage, defective axonal transport, excitotoxicity and inflammation (Boillèe et al., 2006). Damage within motor neurons is enhanced by damage incurred by non-neuronal neighboring cells, via an inflammatory response that accelerates the disease progression (Lobsiger and Cleveland, 2007).

The ALS animal model G93A-SOD1 mouse over expresses the human mutated SOD1 gene and develops a pathology resembling the human disease (Achilli et al., 2005). The G93A-SOD1 mouse is characterized by degeneration of secondary motor neurons in the brain stem and lumbar spinal cord. The onset of the disease appears at week 12 of life with hind limb tremor; at about week 18 of life the animals present muscle paralysis and atrophy of hind limb due to the degeneration of secondary motor neurons of spinal cord, and start to have difficulties in breathing, until they die for respiratory arrest (Achilli et al., 2005). It is unknown the sequence of motor neuron

degeneration resulting in disease. Several studies in the mouse model have shown dysfunction/degeneration of the neuromuscular junction (Frey et al., 2000; Kennel et al., 1996) at times when motor neuron loss is not detected in the mice (Chiu et al.,1995). Furthermore, distal axonopathy was shown to occur early, following neuromuscular junction impairment, but before neuronal degeneration and onset of symptoms (Fischer et al., 2004). Muscle atrophy was shown to precede this sequence of events in the mouse model (Brooks et al., 2004), and recent studies in mice expressing mutant SOD1 gene variants selectively in skeletal muscle suggest that muscle degeneration might itself lead to neurodegeneration and cause ALS (Dobrowolny et al., 2008).

The first aim of the study was to analyze the progression of ALS, by evaluating muscle atrophy and neuronal degeneration in G93A-SOD1 mice. For this purpose, we used the MRI, a non-invasive neuroimmaging tool that permits longitudinal examination of the same animals, to investigate changes in both brain and skeletal muscle at various phases of disease development and progression. We combinated MRI investigation with muscle histological analysis and motor tests to time pathological changes in the brain versus pathological changes in muscle architecture, in relation to clinical signs. Our analysis of T1-weighted images of hind limb muscles showed a significant reduction as early as week 8 in muscle volume of G93A-SOD1 mice, as compared to control mice. Our data indicated that, while early clinical signs first appear around week 12 in G93A-SOD1 mice confirmed through concomitant three way monitoring of clinical disease progression from week 8, disease onset actually occurs

in these mice at least 4 weeks earlier. Our longitudinal histological analysis confirmed the MRI findings; indeed, evidence of muscle atrophy with significant reductions in muscle fiber diameter was observed from week 8 onwards in the G93A-SOD1 mice. Our concomitant longitudinal MRI analysis of the whole brain demonstrated unequivocally that muscular degeneration in G93A-SOD1 mice occurred prior to neurodegeneration. Indeed, clear T2-weighted MRI hyperintensity was only detected at week 10, whereas significant alterations were observed in the muscle at week 8. Our longitudinal study demonstrated clear muscular alterations before any evidence of neurodegeneration and clinical signs in the ALS murine model. Our findings further corroborated the hypothesis that in the murine model of ALS, neurodegeneration resulting from muscular degeneration occurs through a retrograde “dying-back” mechanism (Wong and Martin, 2010). Future studies will be aimed to better support this hypothesis through the analysis of neurodegeneration that occur the spinal cord of G93A-SOD1 mice by MRI longitudinal study. We will perform longitudinal examination of G93A-SOD1 mice and controls, to investigate changes in spinal cord at various phases of disease development and progression. This study will permit to identify the first target of disease.

Based on several studies that demonstrated the presence of stem cells in human and rodent adult spinal cord suggesting that endogenous stem cells might be exploited to repair or sustain the neurodamage or might be a relevant source of multipotent cells to investigate disease mechanisms and evaluate potential therapies (Danilov et al., 2006; Haidet-Phillips et al., 2011; Chi et al., 2005), in the second part of the

thesis we evaluated: if the adult spinal cord of G93A-SOD1 mice was a potential source of stem cells, if stem cells derived from spinal cord have a wild- type phenotype and finally, if miRNA expression was altered during the neural differentiation of these stem cells. For this propose, we first identified nestin positive cells in spinal cord tissue of G93A-SOD1 mice at asymptomatic and symptomatic phase of disease and from control animals; next, we isolated and characterized the stem cells *in vitro*; finally, we analyzed four specific miRNAs, miR-124a and -9 and miR-19a and -19b, in stem cell population and in spinal cord tissue. Our data showed a greater number of nestin positive stem cells in the spinal cord of G93A-SOD1 mice compare to controls. The isolated stem cells maintained *in vitro* their proliferative and self-renewal capacity when the passage increased in culture. Indeed, our *in vitro* studies revealed that differentiated G93A-SOD1 stem cells produced more neurons and fewer astrocytes than controls, and the proportion of neurons further increased (and of astrocytes decreased) in late stage disease, suggesting that neural fate programming might be altered in G93A mice. The G93A-SOD1 astrocytic cells were more activated (thicker processes and greater GFAP immunoreactivity) (Escatin and Bonvento, 2008) than differentiated control cells, at both asymptomatic and symptomatic time points. As regards neurons differentiated from G93A-SOD1 stem cells, those isolated at week 18 were significantly smaller than those from control. Our hypothesis that neural fate programming is altered in G93A-SOD1 mice is reinforced by changes in miR-9, miR-124a and miR-19a expression levels on derived-spinal cord stem cells differentiated *in vitro*. These miRNAs were highly up-regulated in differentiated G93A-SOD1 stem cells

isolated at week 18 compared to week 8, whereas changes in expression following differentiation of control stem cells were minimal. In G93A-SOD1 spinal cord tissue miR-9 and miR-124a expression was highly down-regulated in comparison with controls, in contrast to our findings on differentiated cells *in vitro* (where miR-9 and miR-124a was highly up-regulated). While miR-19a and miR-19b expression was up-regulated in the G93A-SOD1 mouse spinal cord in comparison with controls. Our data are consistent with the greater number of nestin positive cells and the few sporadic neuroblast cells that we observed in week 18 G93A-SOD1 spinal cord tissue.

Future studies will be aimed to better confirm the role of these four miRNAs on derived-spinal cord stem cells differentiated *in vitro*. Based on miRNA target prediction we will analyze the expression of PTEN, Ccnd2, Socs1, Stat3, Stmn1, Hs1, Nr21, Sox9, Jag1, Dlx2 genes in stem cell population and in spinal cord tissue. Moreover, we will better define the functionality of miRNAs, mimicking or inhibiting their expression *in vitro* cultures and *in vivo* in the ALS animal model. These future studies will further support our hypothesis that neural fate programming is altered in G93A-SOD1 mice due to changes in miRNA expression during differentiation of spinal cord-derived stem cells.

REFERENCES

Achilli F, Boyle S, Kieran D, Chia R, Hafezparast M, Martin JE, Schiavo G, Greensmith L, Bickmore W, Fisher EM. (2005). The SOD1 transgene in the G93A mouse model of amyotrophic lateral sclerosis lies on distal mouse chromosome 12. Amyotroph Lateral Scler Other Motor Neuron Disord 6:111-114.

Andersen PM, Al-Chalabi A. (2011). Clinical genetics of amyotrophic lateral sclerosis: what do we really know? Nat Rev Neurol 7:603-615.
Anderson CM, Swanson RA. (2000). Astrocyte glutamate transport: review of properties, regulation, and physiological functions. Glia 32:1-14.

Boillèe S, Vande CV, Cleveland DW. (2006). ALS: A disease of motor neurons and their nonneuronal neighbors. Neuron 52:39-59.

Brooks KJ, Hill MD, Hockings PD, Reid DG. (2004). MRI detects early hindlimb muscle atrophy in Gly93Ala superoxide dismutase-1 (G93A SOD1) transgenic mice, an animal model of familial amyotrophic lateral sclerosis. NMR Biomed 17:28-32.

Chi L, Ke Y, Luo C, Li B, Gozal D, Kalyanaraman B, Liu R. (2005). Motor neuron degeneration promotes neural progenitor cell proliferation, migration, and neurogenesis in the spinal cords of amyotrophic lateral sclerosis mice. Stem Cells 24:34-43.

Chiu AY, Zhai P, Dal Canto MC, Peters TM, Kwon YW, Prattis SM, Gurney ME. (1995). Age-dependent penetrance of disease in a transgenic mouse model of familial amyotrophic lateral sclerosis. Mol Cell Neurosci 6:349-362.

Danilov AI, Covacu R, Moe MC, Langmoen IA, Johansson CB, Olsson T, Brundin L. (2006). Neurogenesis in the adult spinal cord in an experimental model of multiple sclerosis. Eur J Neurosci 23:394-400.

Dobrowolny G, Aucello M, Rizzuto E, Beccafico S, Mammucari C, Boncompagni S, Bonconpagni S, Belia S, Wannenes F, Nicoletti C, Del Prete Z, Rosenthal N, Molinaro M, Protasi F, Fanò G, Sandri M, Musarò A. (2008). Skeletal muscle is a primary target of SOD1 G93A-mediated toxicity. Cell Metab 8:425-436.

Escartin C, Bonvento G. (2008). Targeted activation of astrocytes: a potential neuroprotective strategy. Mol Neurobiol 38:231-241.

Fischer LR, Culver DG, Tennant P, Davis AA, Wang M, Castellano-Sanchez A, Khan J, Polak MA, Glass JD. (2004). Amyotrophic lateral sclerosis is a distal axonopathy: evidence in mice and man. Exp Neurol 185:232-240.

Frey D, Schneider C, Xu L, Borg J, Spooren W, Caroni P. (2000). Early and selective loss of neuromuscular synapse subtypes with low

sprouting competence in motoneuron diseases. J Neurosci 20:2534-2542.

Gruzman A, Wood WL, Alpert E, Prasad MD, Miller RG, Rothstein JD, Bowser R, Hamilton R, Wood TD, Don W, Cleveland, Lingappa VR, Liu J. (2007). Common molecular signature in SOD1 for both sporadic and familial amyotrophic lateral sclerosis. Proc Natl Acad Sci 104:12524-12529.

Haidet-Phillips AM, Hester ME, Miranda CJ, Meyer K, Braun L, Frakes A, Song S, Likhite S, Murtha MJ, Foust KD, Rao M, Eagle A, Kammesheidt A, Christensen A, Mendell JR, Burghes AH, Kaspar BK. (2011). Astrocytes from familial and sporadic ALS patients are toxic to motor neurons. Nat Biotechnol 29:824-828.

Kennel PF, Finiels F, Revah F, Mallet J. (1996). Neuromuscular function impairment is not caused by motor neuron loss in FALS mice: an electromyographic study. Neuroreport 7:1427-1431.

Lobsiger CS, Cleveland DW. (2007). Glial cells as intrinsic components of non-cell-autonomous neurodegenerative disease. Nat Neurosci 10:1355-1360.

Wong M, Martin LJ.(2010). Skeletal muscle-restricted expression of human SOD1 causes motor neuron degeneration in transgenic mice. Hum Mol Genet 19:2284-2302.

Acknowledgments

This study would not have been possible without a network of colleagues and friends.

I am deeply grateful to Dr. Renato Mantegazza, who gave me the privilege to be a part of his operative unit and always put his trust in my skills.

A special thank to Dr. Pia Bernasconi, who always encouraged me during this engaging scientific travel with her precious advices and support.

I wish to thank Dr. Lauria, mentor of my PhD, who guided me with great enthusiasm towards my ultimate aim.

A very special thank to all my colleagues, Paola Cavalcante, Silvia Bonanno, Lara Colleoni, Cristina Cappelletti, Tiziana Pierro, Claudia Barzago for their generosity and patience; our afternoon and evening breaks have always been creative moments for our discussions.

I wish to thank my “friends of the garden”, who always gave me the chance to escape travelling and living unforgettable moments.

Thanks to “hyenas”, Elena, Ilaria, Graziella and Elisa, who represented my tower of strength in these years.

Simply: thanks mother, father and brother.

Thanks Francesco! Your words, your opinions, your support and your love help me to follow my great passion for research.